To the Graduate Council:

I am submitting herewith a thesis written by Jerad D. Bales entitled "Closed Form Solutions of the Kinematic Streamflow Equations." I recommend that it be accepted in partial fulfillment of the requirements for the degree of Master of Science, with a major in Environmental Engineering.

Donald E. Overton

Donald E. Overton, Major Professor

We have read this thesis
and recommend its acceptance:

William A. Miller Jr.

Accepted for the Council:

L Evans Peck

Vice Chancellor
Graduate Studies and Research

Thes
78
.B344
cop. 2

CLOSED FORM SOLUTIONS OF THE KINEMATIC STREAMFLOW EQUATIONS

A Thesis

Presented for the

Master of Science

Degree

The University of Tennessee, Knoxville

Jerad D. Bales

August 1978

136338

ACKNOWLEDGMENTS

The author wishes to express his gratitude to Dr. Donald E. Overton, major professor and advisor, for his support, interest, and encouragement throughout this study. He also wishes to express his appreciation to the other members of the committee, Dr. Roy O. Ball and Dr. William A. Miller, for their review of this manuscript and helpful comments. The assistance given by fellow graduate student, Mr. Ernest Crosby, is also gratefully acknowledged.

The assistance in data collection given by Mr. Bernie Frederick of the U.S. Geological Survey is appreciated.

ABSTRACT

Although kinematic streamflow had been previously thought of as occurring only under supercritical flow conditions, a recent study has shown that subcritical kinematic streamflow does in fact occur in natural conditions. However, the hydraulic and morphological reasons for this occurrence were not found.

This study is an attempt to gain insight into kinematic streamflow. By integrating the kinematic streamflow momentum equation under certain strict assumptions, a model was developed which allowed the prediction of downstream flow profiles at preselected points in time. Basically, only map data, an inflow hydrograph, and certain parameters which may be simulated are required as input to the models.

The output from the flow models was analyzed for its hydraulic and mathematical significance. It was found that the assumptions under which the models were derived severely limited their practicality. A first generation model was presented, however, which may be used as a basis for further research into the kinematic streamflow phenomenon.

TABLE OF CONTENTS

CHAPTER		PAGE
I.	INTRODUCTION	1
II.	LITERATURE REVIEW	2
	The Kinematic Flow Approximation	2
	Subcritical Kinematic Streamflow	10
	Hydraulic Geometry and Rating Curves	13
III.	METHOD AND PROCEDURE	22
	Data Acquisition	22
	Integration of the Momentum Equation	22
	Derivation of Rating Curves and Resistance Coefficients	29
	Flow Profile Analysis	39
	Simulation Example	44
IV.	DISCUSSION OF RESULTS	60
	Rating Curves and Resistance Coefficients	60
	Flow Profile Analysis	62
	Simulation Example	67
V.	CONCLUSIONS AND RECOMMENDATIONS	68
LIST OF REFERENCES		70
APPENDIX		74
VITA		78

LIST OF TABLES

TABLE		PAGE
1.	Mean Station Values of Hydraulic Geometry Exponents	17
2.	Closed Form Analytical Solutions of the Kinematic Streamflow Equations	28
3.	Best Fit Constants at the Four Gaging Stations for $Q = A_o y^b$	30
4.	Best Fit Coefficients for b = 3.0, 2.5, 2.0, and the Chezy Approximation at the Four Stations	35
5.	Physical Characteristics of Manhantango Creek During the Two Events Analyzed	38
6.	Normalized Kinematic Depth Values on Mahantango Creek for Events Analyzed	64

LIST OF FIGURES

FIGURE		PAGE
1.	Laminar and Turbulent Kinematic Wave Solutions and the Observed Rising Hydrograph	9
2.	Loop Stage-Discharge Rating Curve and Associated Discharge Hydrograph for Attenuating Wave	20
3.	Mahantango Creek Study Reach in Plan and Profile Showing Four Gaging Stations	23
4.	Station Four Hydrographs for Events Analyzed	23
5.	Log Stage vs. Log Discharge for Station No. 1, Storm No. 1 .	31
6.	Log Stage vs. Log Discharge for Station No. 2, Storm No. 1 .	32
7.	Log Stage vs. Log Discharge for Station No. 3, Storm No. 1 .	33
8.	Log Stage vs. Log Discharge for Station No. 4, Storm No. 1 .	34
9.	Comparison of Rating Functions at Station No. 1, Storm No. 1.	40
10.	Comparison of Rating Functions at Station No. 2, Storm No. 1.	41
11.	Comparison of Rating Functions at Station No. 3, Storm No. 1.	42
12.	Comparison of Rating Functions at Station No. 4, Storm No. 1.	43
13.	Complete Flow Profiles for b = 3.0; Reach No. 1, Storm No. 1.	45
14.	Complete Flow Profiles for b = 2.5; Reach No. 1, Storm No. 1.	46
15.	Complete Flow Profiles for b = 2.0; Reach No. 1, Storm No. 1.	47
16.	Partial Flow Profiles for b = 3.0; Reach No. 3, Storm No. 1 .	48
17.	Partial Flow Profiles for b = 2.5; Reach No. 3, Storm No. 1 .	49
18.	Partial Flow Profiles for b = 2.0; Reach No. 3, Storm No. 1 .	50
19.	Partial Flow Profiles for b = 3.0; Reach No. 3, Storm No. 2 .	51
20.	Partial Flow Profiles for b = 2.5; Reach No. 3, Storm No. 2 .	52
21.	Partial Flow Profiles for b = 2.0; Reach No. 3, Storm No. 2 .	53

FIGURE PAGE

22. Log Stage vs. Log Discharge on the West Prong Little Pigeon River 55

23. Comparison of Rating Functions; West Prong Little Pigeon River 56

24. Hydrograph Used in Example Simulation on West Prong Little Pigeon River 58

25. Flow Profiles for b = 2.5; West Prong Little Pigeon River . 59

CHAPTER I

INTRODUCTION

Prediction of the movement of a flood wave down a natural channel is essential in the design of channel improvements and flood control measures. Commonly referred to as flood or storm routing, these techniques are also useful in providing input to water quality models.

Most commonly used routing techniques are based on some type of assumed inflow-outflow relationship or on a numerical solution to the full equations of motion. An analytical solution of the equations of motion should provide a routing procedure which is theoretically sound and which requires only a small amount of actual input data.

Because analytical solutions of the full equations of motion are mathematically quite difficult, several approximations to the full equations have been made. The kinematic flow approximation has proved to be a very useful simplification in the determination of the movement of a flood wave down a channel and the prediction of any related changes in form or height of the wave. Although the classical study by Lighthill and Whitham (1) has shown that the kinematic approximation will generally be valid under supercritical flow conditions, Gburek and Overton (2) have shown that subcritical kinematic streamflow does in fact occur.

In this study, the equation for the conservation of linear momentum developed by Gburek and Overton (2) has been integrated, and analytical closed form solutions were found. Based on these solutions, a routing procedure was described, the solutions were analyzed, and, finally, their utility was shown on a test case.

CHAPTER II

LITERATURE REVIEW

The Kinematic Flow Approximation

The approach usually taken in modeling overland and open channel flow is that of a simplified one dimensional flow approximation. The equations expressing conservation of mass and linear momentum in rigid open channels under the conditions of gradually varied unsteady flow are generally known as the de Saint-Venant equations and may be written in several forms. The expression for the conservation of mass in a rectangular channel may be written as

$$\frac{\partial Q}{\partial x} + \frac{\partial A}{\partial t} = q \qquad (1)$$

where

Q = channel discharge;

A = channel cross-sectional area;

x = distance downstream;

t = time; and

q = lateral inflow.

Likewise, the equation for the conservation of linear momentum in a rectangular channel may be expressed as

$$V \frac{\partial V}{\partial x} + \frac{\partial V}{\partial t} + g \frac{\partial y}{\partial x} = g(S_o - S_f) - \frac{Vq}{A} \qquad (2)$$

where

V = velocity;

y = depth of flow;

S_o = bed slope;

S_f = slope of the energy gradient; and

g = acceleration of gravity.

The main problem associated with the use of the full equations of motion has been the difficulty in deriving solutions. Numerous numerical methods have been reported to solve either the full equations of motion or their characteristic equations. The methods based on the solution of the characteristic equations are normally called characteristic methods. Explicit and implicit numerical methods are finite difference schemes used to solve the full equations of motion or the characteristic equations. Explicit methods produce explicit solutions for the dependent variables at a new time level. Implicit methods, on the other hand, solve a set of simultaneous finite difference equations which contain the dependent variables at the new time level (3,4).

The equations of motion may be written in characteristic form as

$$\frac{dQ}{dt} - (V \mp \sqrt{gy}) \frac{dA}{dt} = gA(S_o - S_f) - q(V \mp \sqrt{gy}) \qquad (3)$$

with

$$\frac{dx}{dt} = V \pm \sqrt{gy} \qquad (4)$$

Equation 3 may be integrated along the two sets of characteristic curves given by Equation 4. This method is not limited by the size of the time step but has the major disadvantage of having to interpolate between solution points to provide results at regular time intervals (5). The characteristic equations may also be solved using the finite differencing techniques mentioned previously (6).

Explicit finite-differencing techniques applied to either the characteristic network or to the full equations of flow usually result in linear algebraic equations which may be solved directly. Although explicit methods are generally computationally simple and easy to program, they are only conditionally stable and thus limited in their use to situations with relatively small time steps (3,5).

Implicit schemes, on the other hand, usually do not experience the stability problems that are common to explicit schemes if the implicit difference equations are formulated properly. In addition, some implicit schemes have the advantage of being able to utilize a fixed irregular mesh in the (x,t) plant (7). But, although implicit finite-differencing schemes are normally unconditionally stable and computationally more efficient, they are generally more difficult to program than explicit schemes (3,5).

The mathematical and computational difficulties associated with the numerical or analytical solution of the full equations of motion have led to simplifications of the de Saint-Venant equations. Two approximations to the unsteady flow phenomenon described by the de Saint-Venant equations are the diffusion model and the kinematic model. The diffusion model assumes that the inertia terms in the equations of motion are negligible compared to the pressure, friction, and gravity terms. This model then takes the form

$$\frac{\partial y}{\partial x} = (S_o - S_f) \tag{5}$$

The kinematic wave model assumes that the inertia and pressure terms are negligible compared to the friction and gravity terms (8,10).

The use of the full equations of motion is known as the dynamic wave model. Both the kinematic and diffusion models have been shown to be good approximations to the dynamic model and are finding increased use.

Kinematic wave theory has been well established by researchers such as Lighthill and Whitham (1) and Hyami (9). Kinematic waves occur when the dynamic terms in the momentum equation are negligible, there is no appreciable backwater effect, and discharge is a function of depth along at all x and t.

$$Q = A_o y^b \tag{6}$$

This also implies that the bed slope and slope of the energy gradient are equal (3,11).

The kinematic approximation may be shown by operating on Equation 2, the conservation of linear momentum,

$$\frac{V}{g}\frac{\partial V}{\partial x} + \frac{1}{g}\frac{\partial V}{\partial t} + \frac{\partial y}{\partial x} = (S_o - S_f) - (Vq/gA) \tag{2}$$

Note that the first term in the momentum equation is the convective inertia (convective acceleration) term; the second term represents local (temporal) acceleration; the third term is the pressure differential term; and the fourth term represents bed and friction slopes; the last term accounts for lateral inflow, but is based on continuity rather than momentum considerations. Upon solving for S_f in Equation 2, the momentum expression becomes

$$S_f = S_o\left[1 - \frac{1}{S_o}\left(\frac{V}{g}\frac{\partial V}{\partial x} + \frac{1}{g}\frac{\partial V}{\partial t} + \frac{Vq}{gA}\right)\right] \tag{7}$$

Recall that normal flow may be expressed as

$$Q_n = K\sqrt{S_o} \tag{8}$$

and all one-dimensional flow may be expressed as

$$Q = K\sqrt{S_f} \tag{9}$$

where

K = hydraulic conveyance.

Then Equations 7, 8, and 9 may be combined to give

$$Q = Q_n \left[1 - \frac{1}{S_o} \left(\frac{V}{g} \frac{\partial V}{\partial x} + \frac{1}{g} \frac{\partial V}{\partial t} + \frac{\partial y}{\partial x} + \frac{Vq}{gA} \right) \right]^{1/2} \tag{10}$$

When the dynamic terms, i.e., inertia, pressure, and lateral inflow are small relative to the bed slope, S_o, then the flow is approximately uniform. This means that unsteady flows may be approximated by a series of normal flows using expressions such as the Manning of Chezy formulae.

Henderson (15) has shown that a true wave motion does exist when discharge is a function of depth alone, proving the existence of a kinematic wave. The form of proof employed by Henderson also shows why the term "kinematic" was chosen to describe this type of wave motion. Kinematic wave properties follow principally from the equation of continuity as opposed to the dynamic waves, which arise from the continuity and momentum equations.

The speed of a kinematic wave is given by

$$\frac{dx}{dt} = c = \frac{1}{w} \frac{dQ}{dy} \tag{11}$$

It is important to note that only one wave speed is indicated in Equation 11 for the kinematic wave. Dynamic waves, however, have been shown to have two wave speeds, as indicated by Equation 4, p. 3, The physical significance of this is that kinematic waves will propagate

only in the downstream direction, while dynamic waves move both upstream and downstream (3,11). It has also been shown that kinematic waves move at a speed equal to 1.5 times the mean flow velocity (10,12). This was first observed by Seddon on the Mississippi River in the late nineteenth century (13).

The fact that kinematic waves move only in the downstream direction suggests supercritical flow, Froude number (F) > 1, and the absence of backwater effects. In fact, Lighthill and Whitham (1) have show that at F = 2, the kinematic wave will overtake the dynamic forerunner, and that the dynamic forerunner will rapidly attenuate as it moves downstream. The attenuation of the kinematic wave, however, is zero, i.e., it moves downstream without dissipation, although some distortion of the wave form does occur (10,12).

The kinematic wave approximation has found wide use in applications to overland flow. Woolhiser and Liggett (16), and Henderson and Wooding (17) have presented a solution for the discharge at the end of an initially dry plane, in which the discharge is normalized by the rain rate. Woolhiser and Liggett (16) also introduced the kinematic flow number for turbulent flow over a plane, which was later placed in the following terms (3):

$$k = 10^5 \frac{n^{1.2} S_o^{0.4} L^{0.2}}{i^{0.8}} \qquad (12)$$

where

k = kinematic flow number;

n = Manning roughness coefficient;

S_o = bed slope;

L = length of flow over the plane; and

i = rain rate.

For a k value of 10, it was found that a 10% error would be induced by neglecting the dynamic terms in the solution. The kinematic solution is associated with k values approaching infinity. Thus, as k increases, the error decreases rapidly. In general, large k values are associated with rough, steep, long planes with low rainfall rates (3).

Solutions for the rising hydrograph of flow over long impermeable planes have been presented by several researchers. Overton (18) normalized the rising portion of 214 equilibrium hydrographs measured by the Corps of Engineers over a wide range of rain rates. Scale effects were removed by normalizing the discharge by discharge at equilibrium ($Q*$), and the time by time to equilibrium (t/t_L). It was then found that a single dimensionless rising hydrograph would, within small error, represent all 214 of the normalized hydrographs.

The Manning, Chezy, and laminar kinematic wave models were then compared with the single dimensionless graph. The results are shown in Figure 1. All three models appeared to fit the data well with the Manning-kinematic solution producing a 15% standard error, and the Chezy and laminar models both producing a 19% standard error. It is also significant to note that although flows appear to be laminar on the lower half of the rising hydrograph, only small errors would result if all flows were considered turbulent.

Schreiber and Bender (19) have reported a solution in which the kinematic flow approximation was numerically integrated implicitly (20). A sectional optimization procedure was used to obtain the flow resistance parameters at each hydrograph ordinate. It was later found that two resistance parameters could adequately reproduce the observed hydrographs; one for the rising portion and one for the falling portion of the hydrograph.

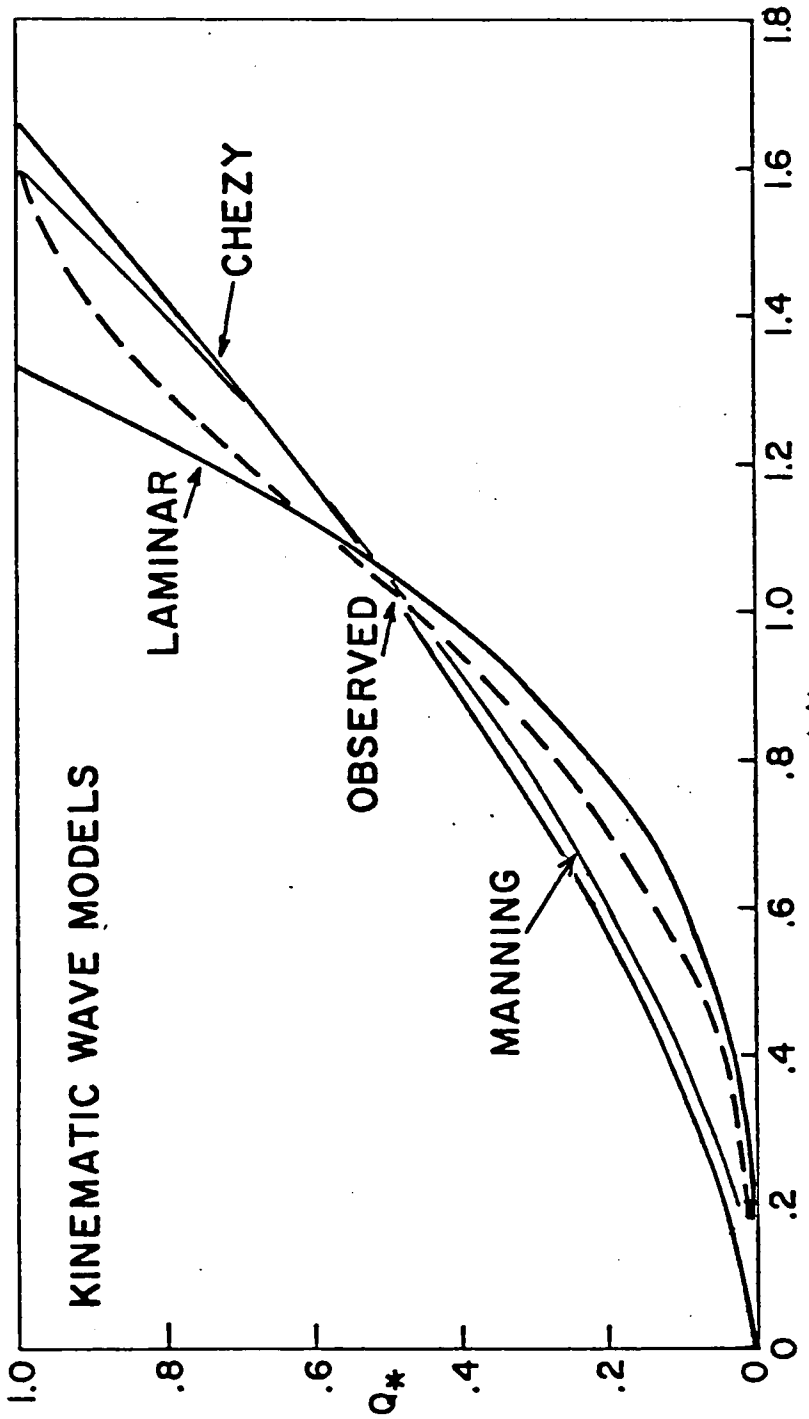


Figure 1. Laminar and Turbulent Kinematic Wave Solutions and Observed Rising Hydrograph. Source: Overton and Meadows (3).

Henderson and Wooding (17) have derived the kinematic equations for the falling overland hydrograph. Solutions were proffered for the case in which the rising hydrograph is at equilibrium, and for the case in which the rainfall duration is less than the time required for the catchment to come to equilibrium.

Various other kinematic overland flow models have been developed for a variety of catchment geometries. Wooding (21) and Overton and Brakensiek (22) have presented models for the V-shaped watershed in which the kinematic flow equations are used to describe the flow on the planes as well as in the channel. Woolhiser (23) developed a model for a converging surface. However, since no general analytical solution has been obtained for the characteristic equations, numerical solutions are required. Finally, Kibler and Woolhiser (24) developed a kinematic flow solution for a cascade of planes.

Subcritical Kinematic Streamflow

Lighthill and Whitham (1) have shown that for F=2, kinematic waves predominate over dynamic waves, and generally a kinematic condition occurs in supercritical flow. However, Gburek and Overton (2) have shown that subcritical kinematic flow conditions existed over a three month storm period on a 7 mile stretch of the Mahantango Creek in eastern Pennsylvania.

After analysis of the data, an expression for the conservation of linear momentum in a wide rectangular channel under conditions of kinematic flow was derived. That derivation will be repeated here for completeness.

Given a single value rating function

$$Q = A_o y^b \tag{13}$$

and the relationship between velocity and discharge as expressed by continuity

$$V = Q/A \tag{14}$$

The following expression results upon substituting Equation 13 into 14 and realizing that A = wy:

$$V = (A_o y^{b-1})/w \tag{15}$$

The partial derivative of velocity with respect to distance is found as follows:

$$\frac{\partial V}{\partial x} = \frac{A_o}{w} \frac{\partial (y^{b-1})}{\partial x} = \frac{A_o y^{b-2}}{w} (b-1) \frac{\partial y}{\partial x} \tag{16}$$

Note the assumption that the channel width remains constant over the reach.

The Froude number may be expressd as

$$F = \frac{V}{\sqrt{c}} = \frac{A_o y^{b-3/2}}{w\sqrt{g}} \tag{17}$$

where c is the wave celerity and equal to $\sqrt{gy}$.

Equations 15, 16 and 17 may now be combined.

$$V \frac{\partial V}{\partial x} \left(\frac{1}{F^2} \right) = (b-1) \frac{\partial y}{\partial x} g \tag{18}$$

or

$$\frac{V}{g} \frac{\partial V}{\partial x} = (b-1) F^2 \frac{\partial y}{\partial x} \tag{19}$$

The time partial of velocity is evaluated next utilizing the definition of the total derivative.

$$\frac{\partial V}{\partial t} = \left[\frac{A_o}{w}(b-1)y^{b-2} \frac{\partial y}{\partial x} \right] \frac{dx}{dt} + \frac{A_o}{w} (b-1)y^{b-2} \frac{\partial y}{\partial t} \qquad (20)$$

Recalling the expression for continuity, Equation 1, p. 2, and the single-valued rating function, Equation 13, p. 11, the partial derivative of discharge with respect to distance may be evaluated. The partial derivative of the cross-sectional area with respect to time may be determined by utilizing the definition of the total derivative and assuming a constant width. The continuity expression then becomes

$$A_o by^{b-1} \frac{\partial y}{\partial x} + w \left(\frac{\partial y}{\partial x} \right) \frac{dx}{dt} + w \frac{\partial y}{\partial t} = q \qquad (21)$$

Solving for $\frac{dx}{dt}$, Equation 21 becomes

$$\frac{dx}{dt} = \frac{q}{w} \left(\frac{\partial x}{\partial y} \right) - \frac{\partial y}{\partial t} \left(\frac{\partial x}{\partial y} \right) - \frac{A_o}{w} by^{b-1} \qquad (22)$$

By substituting Equation 22 into Equation 20, dividing through by g, and substituting in for F, the following expression is obtained:

$$\left(\frac{1}{g} \right) \frac{\partial V}{\partial t} = (A_o q/w^2 g)(b-1)y^{b-2} - b(b-1)F^2 \frac{\partial y}{\partial x} \qquad (23)$$

The first term on the right-hand side of Equation 23 is operated on by multiplying by $(A_o y^{b-1})/w$ and dividing by V. Upon substitution for F^2, the final form of the time partial derivative of velocity becomes

$$\left(\frac{1}{g} \right) \frac{\partial V}{\partial t} = (q/Vw)(b-1)F^2 - b(b-1)F^2 \frac{\partial y}{\partial x} \qquad (24)$$

Equations 19, p. 11, and 24 may now be substituted into the momentum equation, Equation 2, p. 3, resulting in the general expression

for the conservation of linear momentum in a wide rectangular stream under kinematic flow conditions.

$$S_o - S_f = \frac{\partial y}{\partial x}\left[1 - (b-1)^2 F^2\right] + \frac{qb}{Vw} F^2 \qquad (25)$$

Neglecting lateral inflow effects, the momentum relation, Equation 25, becomes

$$S_o - S_f = \frac{\partial y}{\partial x}\left[1 - (b-1)^2 F^2\right] \qquad (26)$$

It can be seen from Equation 26 that the slope of the energy gradient is exactly equal to the bed slope when

$$F = \frac{1}{b-1} \qquad (27)$$

At this point, Lighthill and Whitham (1) have shown that the kinematic and dynamic wave speeds are exactly equal with the kinematic waves assuming the dominant role. Lighthill and Whitham (1) also showed that under these conditions, $F = 2$, and thus, $b = 3/2$. Yet, Gburek and Overton (2) found that while F was never greater than 0.34 during the period of their analysis, the conditions for kinematic flow were met, i.e., the energy gradient and bed slope were very nearly equal, and a single-valued rating function was found to exist over the range of flows encountered in the study. Thus, the occurrence of subcritical kinematic flow conditions was shown.

Hydraulic Geometry and Rating Curves

The concept of hydraulic geometry was first set forth by Leopold and Maddock (25) in their study of over 70 years of streamflow data. The fact that the channel characteristics of natural rivers seemed to constitute

an interdependent system which could be described by a series of graphs having a simple geometric form suggested the term "hydraulic geometry" to Leopold and Maddock. Subsequent studies have verified and expanded upon this initial work with the result that hydraulic geometry equations may be used to provide a general estimate of channel characteristics at any location within the drainage system.

Leopold and Maddock (25), and consequently succeeding researchers, based their studies on the premise that at a given time, all points on a river are experiencing the same frequency of discharge; and, that at a given channel cross section, different discharges have different frequencies. Frequency of discharge is defined as the number of times, on the average, that a given flow will be equaled or exceeded in any given year. Thus a flow with a 10% frequency will, on the average, have a 10% chance of being equaled or exceeded in any given year (26). Based on this premise, the researchers were able to compare different discharges occurring at the same time at different points along a river system.

As a result of their analysis of the variation of hydraulic characteristics at a particular cross section in a river, Leopold and Maddock (25) proposed that discharge be related to other hydraulic factors in the following manner:

$$w = aQ^b \tag{28}$$

$$d = cQ^f \tag{29}$$

$$V = kQ^m \tag{30}$$

where

w = width;

d = depth;

V = mean velocity;

Q = discharge; and

a, b, c, f, k, and m = best fit constants.

It follows that since width, depth, and mean velocity are each functions of discharge, then b, f, and m sum to 1.0; and the product of a, c, and k is 1.0.

After plotting width, depth, and velocity against discharge on log-log paper for 20 river cross sections representing a variety of rivers in the Great Plains and Southwest, Leopold and Maddock (25) found that the slopes of these lines (b, f, and m) were remarkably close in value. But, since width and depth values for a given discharge vary widely from cross section to cross section, the intercept values (a, c, and k) were also found to vary widely among cross sections. The relative changes in width and depth are functions of channel shape. The width-depth ratio remains constant with changing discharge in a triangular shape channel, while the width-depth ratio decreases rapidly with increasing discharge in a rectangular channel.

The average values of the exponents b, f, and m found by Leopold and Maddock (25) are listed below:

$$b = 0.26$$

$$f = 0.40$$

$$m = 0.34$$

The values of f ranged from a high of 0.63 to a low of 0.06. Other researchers have carried out the same analysis on different basins at different times with a noticeable similarity in results. Leopold and Miller (27) studied ephemeral streams, i.e., streams with intermittent

flow, in an area around Sante Fe, New Mexico. They found the same interrelations among hydraulic and physiographic factors in the ephemeral streams as were found for the perrenial streams. Stall and Fok (28) analyzed data from 18 stations on the Sangamon River in Illinois and related the hydraulic factors to the frequency of occurrence of a discharge and to the proportional stream order. Later, Stall and Yang (29) did an extended study of 12 basins in the humid regions of the United States, with each basin representing a different physiographic section of the country. Once again, it was found that the hydraulic geometry of the streams could be expressed by simple power relations such as those used by Leopold and Maddock (25). Finally, the work of Langbein (30) on circulating flumes is found to be in close agreement with other published reports. The information from each of these studies is summarized in Table 1.

Equation 29, p.14, may be rearranged and written in the form of the rating function, Equation 6, p. 5. Equation 29 written with discharge as a function of depth becomes

$$Q = \left(\frac{d}{c} \right)^{1/f} \tag{31}$$

Comparing Equation 31 and Equation 6, it can be seen that

$$A_o = (1/c)^{1/f}$$

$$b = 1/f$$

$$y = d$$

The values for 1/f are also tabulated in Table 1. Note that the range of these values is between 16.67 and 1.59, and that the average value is 3.16.

TABLE 1

MEAN STATION VALUES OF HYDRAULIC GEOMETRY EXPONENTS

Study	River Basin	Width, b	Velocity, m	Depth, f	Discharge, 1/f
Leopold and Maddock[a]	Cheyenne River	0.50	0.25	0.25	4.00
	Middle Loup River	0.32	0.37	0.31	3.23
	Middle Loup River	0.13	0.35	0.52	1.92
	Rio Grande	0.59	0.28	0.13	7.69
	Rio Grande	0.22	0.30	0.48	2.08
	Rio Grande	0.03	0.51	0.46	2.17
	Smoky Hill River	0.36	0.16	0.48	2.17
	Smoky Hill River	0.14	0.26	0.60	1.67
	Powder River	0.10	0.31	0.59	1.69
	Moreau River	0.10	0.34	0.56	1.79
	White River	0.30	0.07	0.63	1.59
	Belle Fourche River	0.31	0.25	0.44	2.27
	Virgin River	0.26	0.45	0.29	3.45
	Rio Puerco	0.43	0.41	0.16	6.25
	Saline River	0.37	0.25	0.38	2.63
	Republican River	0.50	0.44	0.06	16.67
	Bighorn River	0.06	0.43	0.51	1.96
	Bighorn River	0.14	0.55	0.31	3.23
	Bighorn River	0.22	0.28	0.50	2.00
	Grand River	0.25	0.39	0.36	2.78
Leopold and Miller[b]	Average of 7 Ephemeral Streams	0.22	0.35	0.43	2.33
Stall and Yang[c]	Merrimack River	0.20	0.45	0.35	2.86
	Susquehanna River	0.23	0.40	0.37	2.70
	Roanoke River	0.12	0.41	0.47	2.13
	Big Sandy River	0.23	0.36	0.41	2.44

TABLE 1. Continued

Study	River Basin	Exponents			
		Width, b	Velocity, m	Depth, f	Discharge, 1/f
Stall and Yang[c]	White River	0.29	0.35	0.36	2.78
	Sangamon River	0.28	0.23	0.44	2.04
	Neches River	0.35	0.18	0.47	2.13
	Colorado River	0.19	0.45	0.36	2.78
	Tuolumne River	0.30	0.36	0.34	2.94
	Skagit River	0.13	0.52	0.35	2.86
	Snake River	0.11	0.48	0.41	2.44
	Rogue River	0.13	0.53	0.34	2.94
Langbein[d]	Circulating Flume	0.53	0.10	0.37	2.70
Average Values		0.26	0.35	0.39	3.16

[a]Leopold and Maddock (25).

[b]Leopold and Miller (27).

[c]Stall and Yang (24).

[d]Langbein (30).

It should also be noted that the 1/f values taken from the work of Stall and Yang (29) range from 2.04 to 2.94 with an average value of 2.59.

Unfortunately, there cannot be a unique stage-discharge relationship for a given channel cross section as is expressed by Equation 6, p. 5, and Equation 29, p. 14, except for uniform flow conditions. For a given depth, the discharge will be greater during the rising stage of the flood wave than during the falling stage. This loop function is shown in Figure 2. Note that for an attenuating wave, an observer on the bank first sees the point of maximum discharge, then the point of maximum depth, and, finally, a flow which is momentarily uniform (11). It may also be recognized that while an attenuating wave transverses the loop in a clockwise direction, the loop is transversed in a counterclockwise direction if the wave is amplifying. The point of maximum depth would then be on the rising limb of hydrograph followed by the point of maximum discharge. Attenuation of a wave is caused when the discharge in front of the wave is larger than the discharge following the wave. Conversely, if the discharge following the wave is larger than the discharge leading the wave, the wave is compressed and the peak is raised (31).

Since the kinematic wave is approximated by a series of uniform flows, a single-valued rating is required for the kinematic approximation to be valid, i.e., discharge must be a function of depth alone at all x and t. But, if the discharge rating remains constant at a section during a flood, the wave must pass through the section without any peak variation, and all points at the same depth on the hydrograph would move

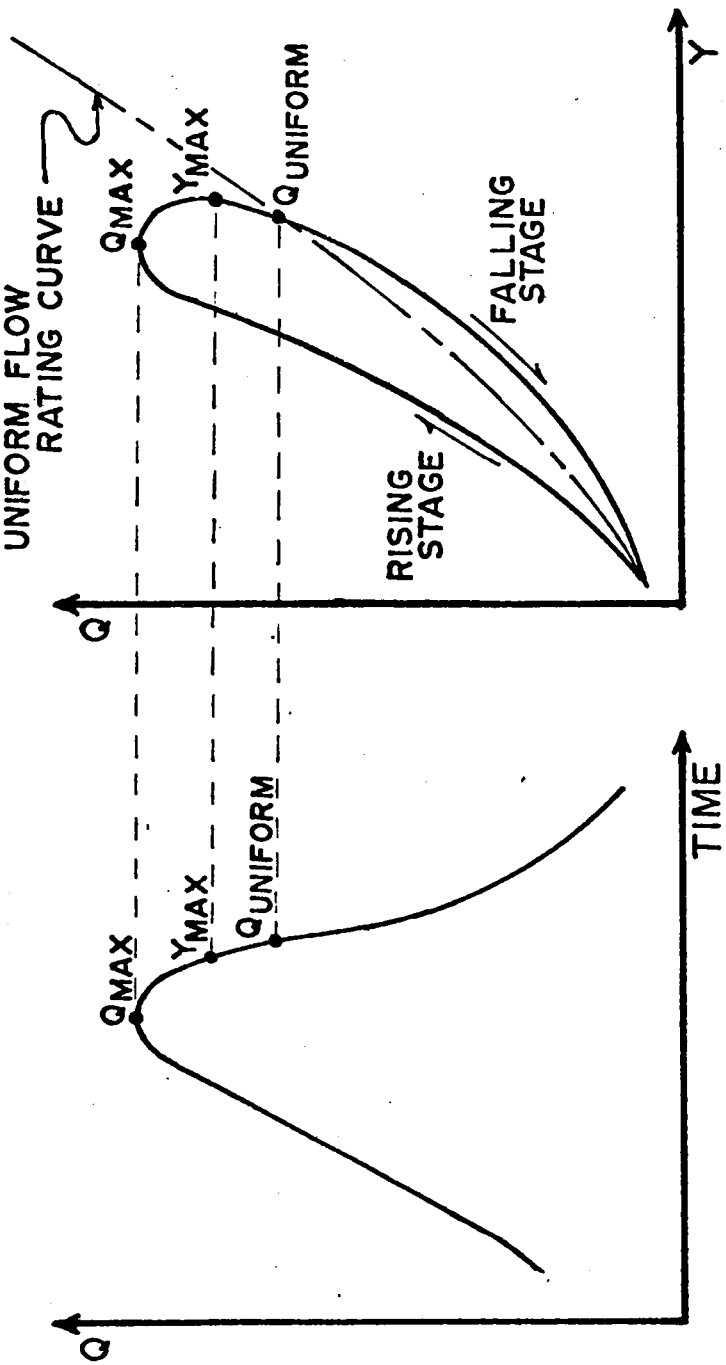


Figure 2. Loop Stage-Discharge Rating Curve and Associated Discharge Hydrograph for Attenuating Wave.

with the same speed. This may result in the wave distoring as it moved downstream, but no attenuation or amplification would occur. In general, however, the passage of the flood wave is not exactly equal to the uniform flow rating curve. Because the dynamic terms neglected in the kinematic wave approximation may be small, but seldom zero, the discharge corresponding to a given stage is usually different during the rising and falling limbs of the hydrograph. The result, then, is that the discharge rating curve may show the loop function even when the kinematic flow approximation is valid. Often, however, the loop effect is small enough to be considered negligible (15, 31).

CHAPTER III

METHOD AND PROCEDURE

Data Acquisition

Data used in the analysis of the closed form analytical solutions of the momentum equation for kinematic streamflow, Equation 25, were the same used by Gburek and Overton (2). The 162 square mile Mahantango Creek Watershed is located in the ridge and valley region of east central Pennsylvania and is drained by the East Mahantango Creek, which flows directly into the Susequehanna River. The plan and profile of the study reach are shown in Figure 3.

Flow depth, cross sectional flow area, and velocity hydrographs were obtained at each of the 4 gaging stations shown in Figure 3. This data was reduced to 2 hour averages for study. Storms selected for study occurred between July 26 and August 14, 1969 (Storm No. 1), and from November 7 to November 27, 1969 (Storm No. 2). These events consisted of 240 and 252 data points, respectively. The discharge hydrographs at the downstream station for the events analyzed are shown in Figure 4.

Integration of the Momentum Equation

The equation for the conservation of linear momentum for kinematic streamflow was derived in Chapter II as

$$S_o - S_f = \frac{\partial y}{\partial x}\left[1 - (b - 1)^2 F^2\right] + \frac{qb}{Vw} F^2 \qquad (25)$$

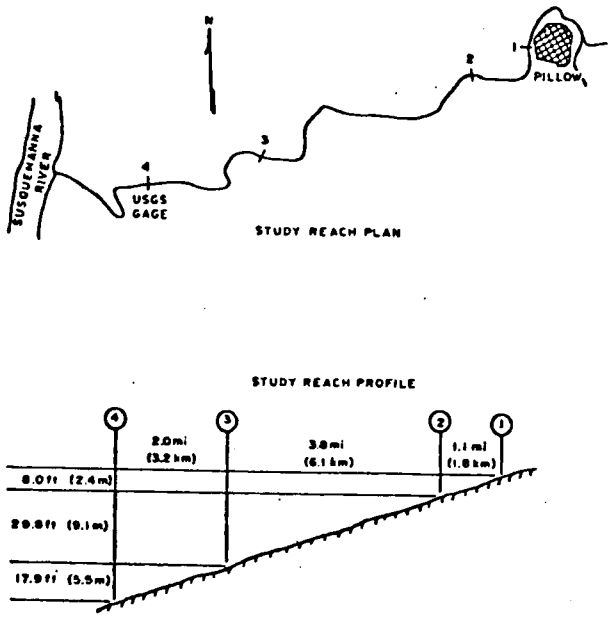


Figure 3. Mahantango Creek Study Reach in Plan and Profile Showing Four Gaging Stations; Source: Gburek and Overton (2).

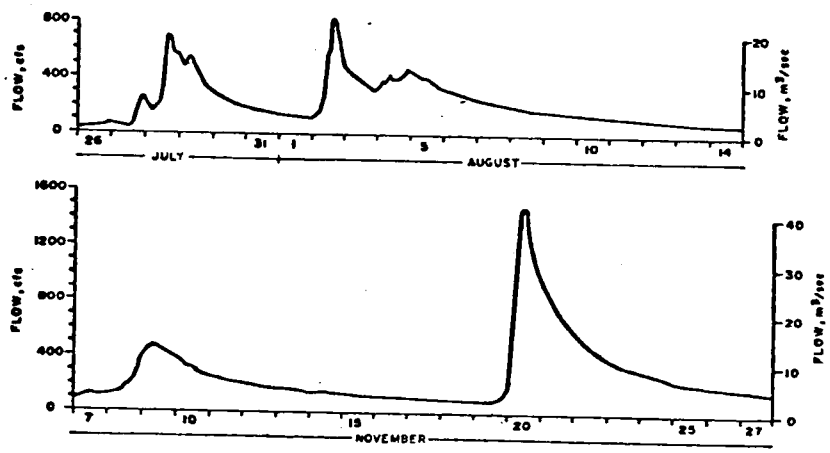


Figure 4. Station Four Hydrographs for Events Analyzed. Source: Gburek and Overton (2).

This equation may be placed in the form of the classical gradually varied flow formula.

$$\frac{\partial y}{\partial x} = \frac{S_o - S_f - \frac{qb}{Vw} F^2}{[1 - (b - 1)^2 F^2]} \tag{32}$$

To obtain closed form analytical solutions of Equation 32, several assumptions must be made. Based on the findings of Leopold and Maddock (25) and particularly on the work of Stall and Yang (29), it was determined that Equation 32 would be solved for the cases of b = 2.0, b = 2.5, and b = 3.0. It may be recalled that Stall and Yang (29) found b-values ranging from 2.04 to 2.94 in their studies of 12 rivers representing 12 physiographic regions in the humid areas of the United States. Starting from this initial assumption, the procedure for the integration of Equation 32 with b, the exponent on the stage-discharge rating function, set equal to 2.5 is set forth below. The integration for the other two cases may be found in the Appendix.

The following relations may be recalled from Chapter II.

$$Q = A_o y^b \tag{6}$$

$$V = \frac{A_o y^{b-1}}{wy} \tag{15}$$

$$F = \frac{A_o y^{b-3/2}}{w\sqrt{g}} \tag{17}$$

Thus Equation 32 becomes

$$\frac{\partial y}{\partial x} = \frac{S_o - S_f - y^{b-2} (qbA_o/w^2 g)}{1 - (b-1)^2 (A_o^2 y^{2b-3}/w^2 g)} \tag{33}$$

The Chezy formula for uniform flow in a wide rectangular channel in which the hydraulic radius may be approximated by the depth, may be written as

$$S_f = \frac{A_o^2 y^{2b-3}}{C^2 w^2} \tag{34}$$

Thus, Equation 33 becomes

$$\frac{\partial y}{\partial x} = \frac{S_o - (A_o^2 y^{2b-3}/C^2 w^2) - y^{b-2} (qbA_o/w^2 g)}{1 - (b-1)^2 (A_o^2 y^{2b-3}/w^2 g)} \tag{35}$$

Substituting in for b = 2.5 and assuming that the lateral inflow is negligible results in

$$\frac{\partial y}{\partial x} = \frac{S_o - (A_o^2 y^2/C^2 w^2)}{1 - 2.25 (A_o^2 y^2/w^2 g)} \tag{36}$$

Upon separation of variables, Equation 36 becomes

$$\int \partial x = \frac{1}{(A_o/Cw)^2} \int \frac{\partial y}{\left(\frac{S_o}{(A_o/Cw)^2}\right) - y^2} - \frac{2.25\ C^2}{g} \int \frac{y^2 \partial y}{\left(\frac{S_o}{(A_o/Cw)^2}\right) - y^2} \tag{37}$$

If the stage discharge rating function and the Chezy uniform flow formula are set equal, the following result is obtained for a wide rectangular channel:

$$A_o y^b = Cw y_n^{3/2} S_o^{1/2}$$

or

$$\frac{y^b}{y_n^{3/2}} = \frac{Cw}{A_o} S_o^{1/2} \tag{38}$$

Define the new term y_n^* as

$$y_n^* = \frac{y}{y_n} = \left(\frac{Cw}{A_o} S_o^{1/2} \right)^{1/(b-3/2)} \tag{39}$$

Substituting for b = 2.5, y_n^* is now

$$y_n^* = \frac{S_o^{1/2}}{A_o/Cw} \tag{40}$$

and

$$y_n^* = \frac{S_o}{(A_o/Cw)^2} \tag{41}$$

This convenient form may now be substituted back into Equation 37.

$$\int \partial x = \frac{y_n^{*2}}{S_o} \int \frac{\partial y}{y_n^{*2} - y^2} - \frac{2.25\ C^2}{g} \int \frac{y^2 \partial y}{y_n^{*2} - y^2} \tag{42}$$

After further algebraic manipulation, in which the assumption is made that y_n^* is constant over a reach, Equation 42 becomes

$$\int \partial x = \frac{y_n^{*2}}{S_o} \int \frac{\partial(y/y_n^*)}{1 - (y^2/y_n^{*2})} - \frac{2.25\ C^2 y_n^*}{g} \int \frac{(y^2/y_n^{*2})\partial(y/y_n^*)}{1 - (y^2/y_n^{*2})} \tag{43}$$

Since the momentum equation was derived for subcritical kinematic streamflow, the two boundary conditions are taken at each end of the channel reach (33). The upstream boundary condition is the inflow depth hydrograph, or

$$\text{at } x = 0,\ y = y(0,t)$$

The downstream boundary conditions is the known rating function,

$$Q = A_o y^b \ .$$

Thus, the final integrated form of the momentum equation for the case of b = 2.5 may be given by

$$x = (2.25\ C^2 y_n^*/g)(U-U_o) + 0.5\ y_n^* [(1/S_o) - 2.25\ C^2/g)]* \log\left[\left(\frac{1+U}{1-U}\right)\left(\frac{1-U_o}{1+U_o}\right)\right] \tag{44}$$

where

$$U = y(x,t)/y_n^* \quad ; \quad \text{and}$$

$$U_o = y(0,t)/y_n^* \quad .$$

The integrated momentum equations for the three cases of b = 2.0, b = 2.5, and b = 3.0 are shown in Table 2. Note that for the case of b = 2.0, the lateral inflow term has been included, and it may be input into the integrated equation as a step function. With b = 2.0, the lateral inflow term becomes a constant and thus may be included in the solution. However, for the cases of b = 2.5 and b = 2.0, the lateral inflow term must be integrated. Closed form analytical solutions could not be found for these cases. Note also that for b = 3.0, the term inside the brackets may be written as the well known Bresse function.

$$\Phi - \Phi_o = \left(\frac{1}{6}\ln\left[\frac{U^2 + U + 1}{(U-1)^2}\right] - \frac{1}{\sqrt{3}}\tan^{-1}\left[\frac{\sqrt{3}}{2U+1}\right]\right) - \left(\frac{1}{6}\ln\left[\frac{U_o^2 + U_o + 1}{(U_o - 1)^2}\right] - \frac{1}{\sqrt{3}}\tan^{-1}\left[\frac{\sqrt{3}}{2U+1}\right]\right) \qquad (45)$$

where Φ is Bresse's function.

To summarize, the assumptions under which the equations in Table 2 were derived will be listed below.

1. The momentum equation, Equation 25, was derived for turbulent subcritical kinematic streamflow in a stable stream. This implies the existence of a single-valued rating function, and that a uniform flow formula, such as Manning's or Chezy's may be extrapolated to describe the unsteady, non-uniform flow taking place.

TABLE 2

CLOSED FORM ANALYTICAL SOLUTIONS OF THE
KINEMATIC STREAMFLOW EQUATIONS

b Value	Solution
2.0	$x = (C^2 y_n^*/g)(U-U_o) + y_n^*[(C^2/g) - (1/S_o) - (2qC^2A_o/w^2g^2S_o)] \log \left[\frac{1 - (2qA_o/w^2gS_o) - U}{1 - (2qA_o/w^2gS_o) - U_o} \right]$
2.5	$x = (2.25\ C^2 y_n^*/g)(U-U_o) + 0.5\ y_n^*[(1/S_o) - (2.25\ C^2/g)] \log \left[\frac{(1 + U)(1 - U_o)}{(1 - U)(1 + U_o)} \right]$
3.0	$x = (4C^2 y_n^*/g)(U - U_o) + y_n^* [(1/S_o) - (4C^2/g)] \left[\frac{1}{6} \ln \left[\frac{U^2 + U + 1}{(U - 1)^2} \right] \left[\frac{(U_o - 1)^2}{U_o^2 + U_o + 1} \right] - \frac{1}{\sqrt{3}} \left[\tan^{-1} \left(\frac{\sqrt{3}}{2U + 1} \right) - \tan^{-1} \left(\frac{\sqrt{3}}{2U_o + L} \right) \right] \right]$

2. The channel was assumed to be wide rectangular such that the hydraulic radius is closely approximated by the depth of flow.
3. The exponent on the rating curve was assumed to be either 2.0, 2.5, or 3.0. These values were chosen on the basis of the work of Stall and Yang (24) and for their computational tractability.
4. The term y_n^* was assumed constant over the reach. This implies that the bed slope, width, resistance coefficient and the constant on the rating curve, A_o, are all constant over the reach. This stipulation was incorporated by averaging the upstream and downstream conditions, and assuming that this average condition applied all along the reach.
5. Although the Chezy uniform flow formula was used in this derivation, the integrations may also be carried out using the Manning approximation to uniform flow.
6. The integrated equations apply to in-bank conditions only.

Derivation of Rating Curves and Resistance Coefficients

To obtain a relationship between discharge and depth, Gburek and Overton (2) fit the data from the two storms to the power relation

$$Q = A_o y^b \quad . \tag{6}$$

The best fit constants which they found for each of the 4 stations over the range of flows analyzed are shown in Table 3. Note that the

TABLE 3

Best Fit Constants at the Four Gaging Stations for $Q=A_o y^b$

Station	b	A_o	r^2
1	2.74	14.70	0.99
2	3.39	7.09	0.98
3	3.29	40.90	0.98
4	3.02	17.90	0.99

Source: Gburek and Overton (2).

b values fell within the range suggested by Leopold and Maddock's (25) work. Log discharge is plotted against log depth in Figures 5 through 8 at each of the 4 gaging stations for Storm No. 1. The best fit lines with a slope equal to b and intercept equal to log A_o are also shown.

In order to utilize the integrated momentum equations, the Mahantango Creek (2) data was reanalyzed. The values of the exponent on the rating curve, b, were set at b = 3.0, 2.5, and 2.0. A linear regression was then performed on the data resulting in A_o values at each station and for each b value. These results are shown in Table 4 for Storm No. 1 and Storm No. 2.

Chezy C values were optimized at each station and for each storm using the least squares method reported by Overton (34) as applied to rectangular flumes. This method was later applied by Yen and

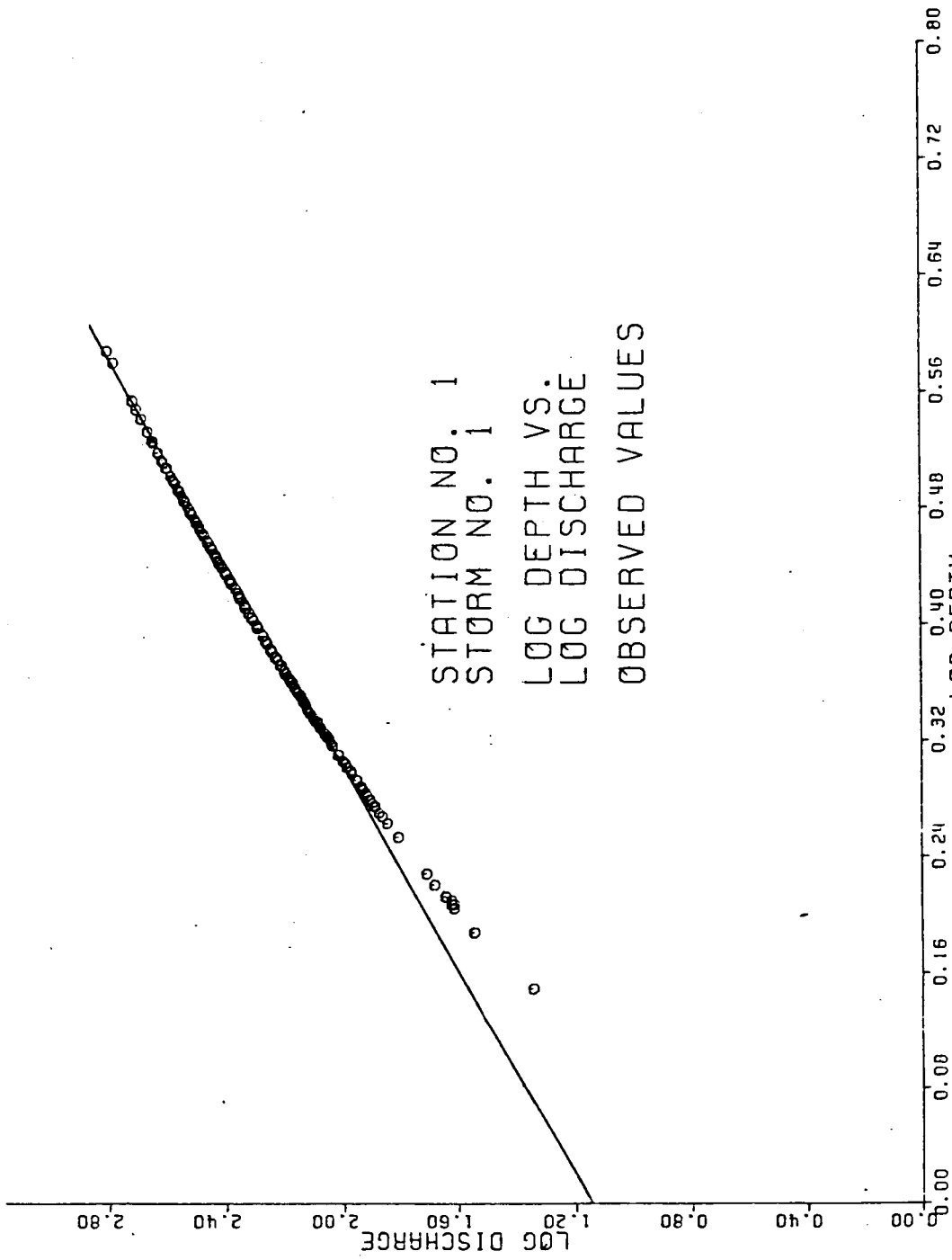


Figure 5. Log Stage vs. Log Discharge for Station No. 1, Storm No. 1.

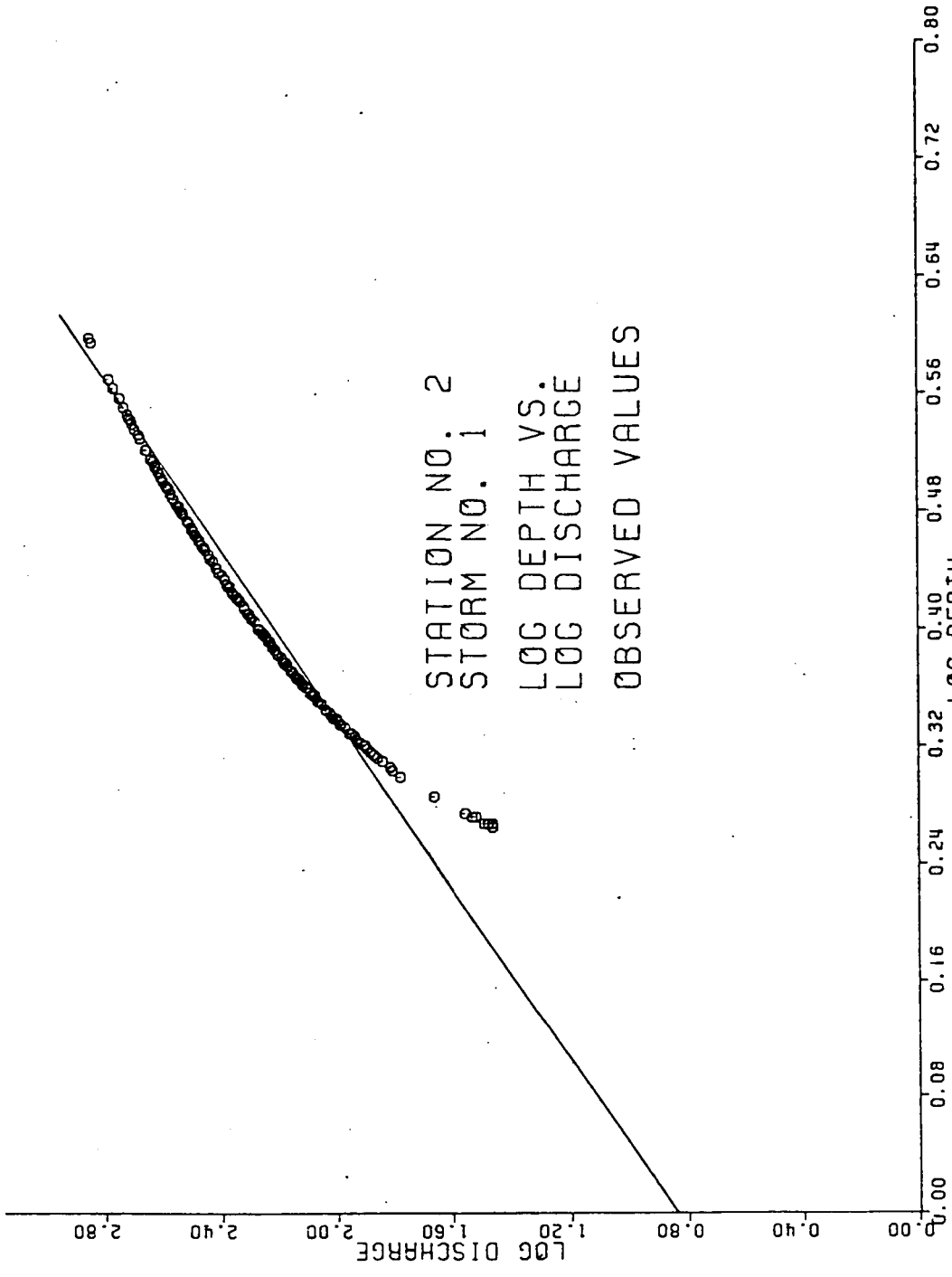


Figure 6. Log Stage vs. Log Discharge for Station No. 2, Storm No. 1.

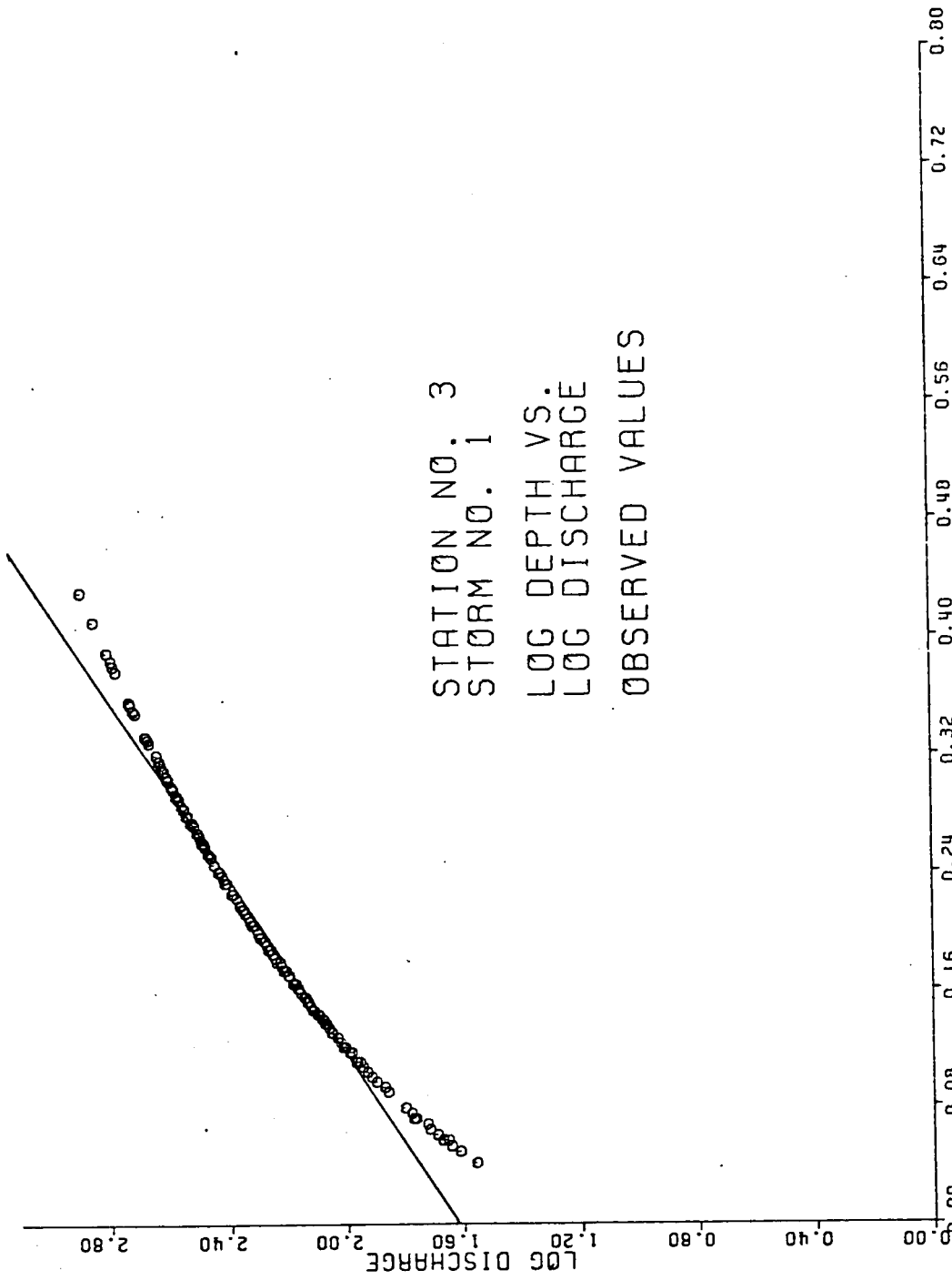


Figure 7. Log Stage vs. Log Discharge for Station No. 3, Storm No. 1.

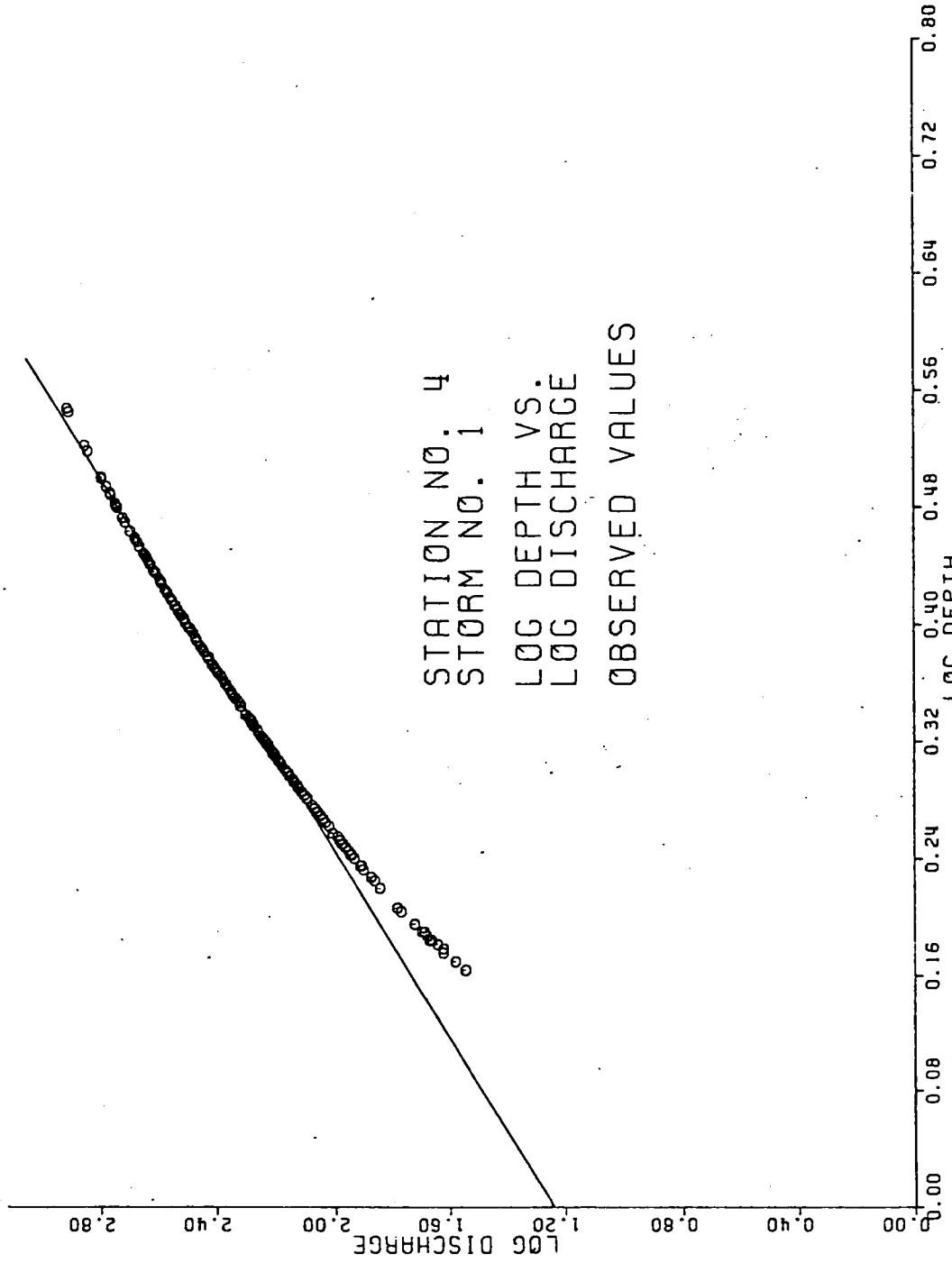


Figure 8. Log Stage vs. Log Discharge for Station No. 4, Storm No. 1.

TABLE 4

BEST FIT COEFFICIENTS FOR b = 3.0, 2.5, 2.0, AND THE CHEZY APPROXIMATION AT THE FOUR STATIONS

Station	Storm No. 1			Storm No. 2		
	b	A_o	r^2	b	A_o	r^2
1	3.0	11.81	0.99	3.0	11.66	0.98
	2.5	18.03	0.97	2.5	18.25	0.97
	2.0	27.81	0.92	2.0	28.89	0.89
	1.5[a]	53.08[b]	0.84	1.5[a]	59.88[b]	0.83
2	3.0	10.15	0.96	3.0	10.31	0.98
	2.5	16.20	0.91	2.5	16.82	0.94
	2.0	26.05	0.85	2.0	27.75	0.85
	1.5[a]	53.42[b]	0.83	1.5[a]	59.47[b]	0.86
3	3.0	46.60	0.79	3.0	46.99	0.92
	2.5	58.77	0.97	2.5	60.33	0.99
	2.0	74.78	0.92	2.0	78.64	0.89
	1.5[a]	111.64[b]	0.86	1.5[a]	124.23[b]	0.88

TABLE 4. Continued

Station	Storm No. 1			Storm No. 2		
	b	A_o	r^2	b	A_o	r^2
4	3.0	18.18	0.99	3.0	18.20	0.92
	2.5	26.86	0.95	2.5	27.58	0.96
	2.0	40.07	0.89	2.0	42.34	0.87
	1.5[a]	73.71[b]	0.84	1.5[a]	84.23[b]	0.85

[a]Chezy approximation.

[b]$A_o = Cw\sqrt{S_o}$.

Overton (35) to channel-flood plain geometries, and by Overton (36) to overland flow surfaces. To optimize C, a line was fit through a plot of discharge versus width times depth raised to the 3/2 power times the square root of the bed slope. The optimization was performed such that the y-intercept of this line would be through the origin. Thus, the slope of the line was the Chezy-C value. Algebraically this is

$$Q = C(wy^{3/2}\sqrt{S_o}) + a \tag{46}$$

where

a = intercept of the Q vs. $(wy^{3/2}\sqrt{S_o})$ line, in this case a = 0; and

C = slope of the Q vs. $(wy^{3/2}\sqrt{S_o})$ line, the Chezy-C value.

The C values at each station and for each storm are tabulated in Table 5. If the Chezy relation for a wide rectangular channel

$$Q = Cwy^{3/2}\sqrt{S_o} \tag{47}$$

were to be written in the form of the rating curve, Equation 6, it can be seen that b would equal 3/2 and

$$A_o = Cw\sqrt{S_o} \tag{48}$$

These A_o values and the coefficient of determination, r^2, showing the goodness of fit of the Chezy approximation to the observed discharges are also shown in Table 4.

A stage-discharge rating curve was calculated at each station for the cases of b = 3.0, b = 2.5, b = 2.0; and using the optimized C-values in the Chezy approximation. These 4 rating curves, along with the observed data and the best fit curves determined by Gburek and

TABLE 5

PHYSICAL CHARACTERISTICS OF MAHANTANGO CREEK DURING THE TWO EVENTS ANALYZED

Property	Storm No. 1				Storm No. 2			
Station No.	1	2	3	4	1	2	3	4
	20.62	24.54	34.05	28.81	23.26	27.32	37.89	32.92
Average w(ft.)	68.81	58.39	81.97	60.14	70.72	59.57	82.79	61.48
Average y(ft.)	2.38	2.53	1.59	2.20	2.51	2.65	1.65	2.32
Average R(ft.)	2.22	2.33	1.53	2.05	2.34	2.43	1.58	2.16
Bed Slope (ft./ft.)	0.00136	0.00139	0.00160	0.00181	0.00136	0.00139	0.00160	0.00181

Overton (2), are shown in Figures 9 through 12 at each of the 4 stations for Storm No. 1.

Average width, depth, and hydraulic radius values found by averaging over the duration of the storm at each station are shown in Table 5, p. 38. Average width values are necessary to meet the stipulation used in the integration that the width be constant over a reach. Average depth and hydraulic radius values at each station are intended to show that the assumption that the hydraulic radius may be approximated by the depth is indeed valid. Bed slope values were obtained from Gburek and Overton (2).

Flow Profile Analysis

Flow profiles, a plot of depth versus distance downstream, were developed using the integrated momentum equations in Table 2, p. 27. By averaging the width, bed slope, Chezy-C, and rating curve coefficient, A_0, at the upstream and downstream stations, an average condition was found for each reach during each storm. This average condition was assumed to remain constant throughout the duration of an event.

Since the integrated equations are highly nonlinear with respect to y, a numerical scheme was employed to solve the equations. By substituting into the equations an incremental distance downstream, the inflow hydrograph, y(0,t), and the average physical characteristics of the reach, the depth at the incremental distance downstream could be solved for at all values of time. The distance parameter was then increased and the process

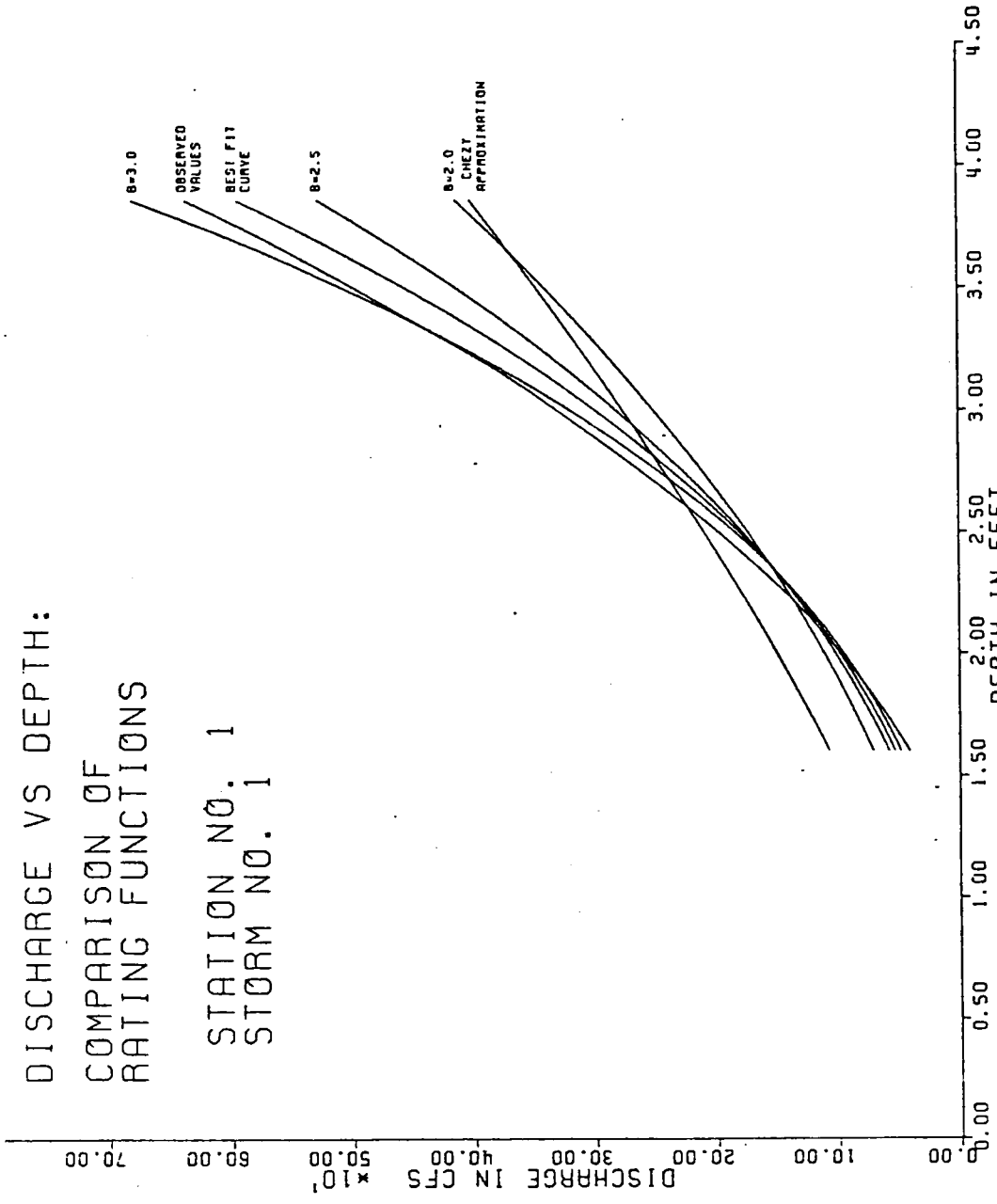


Figure 9. Comparison of Rating Functions at Station No. 1, Storm No. 1.

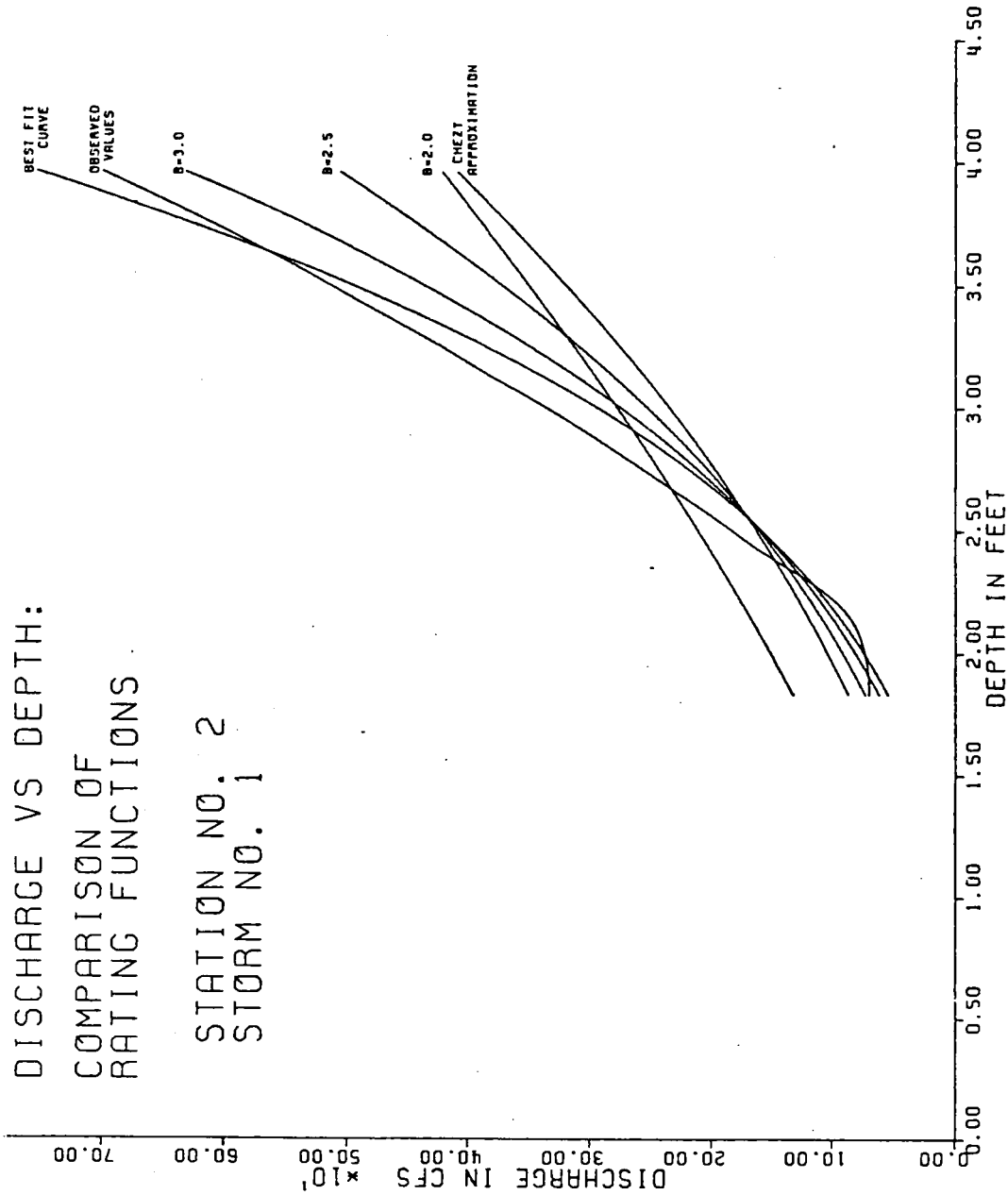


Figure 10. Comparison of Rating Functions at Station No. 2, Storm No. 1.

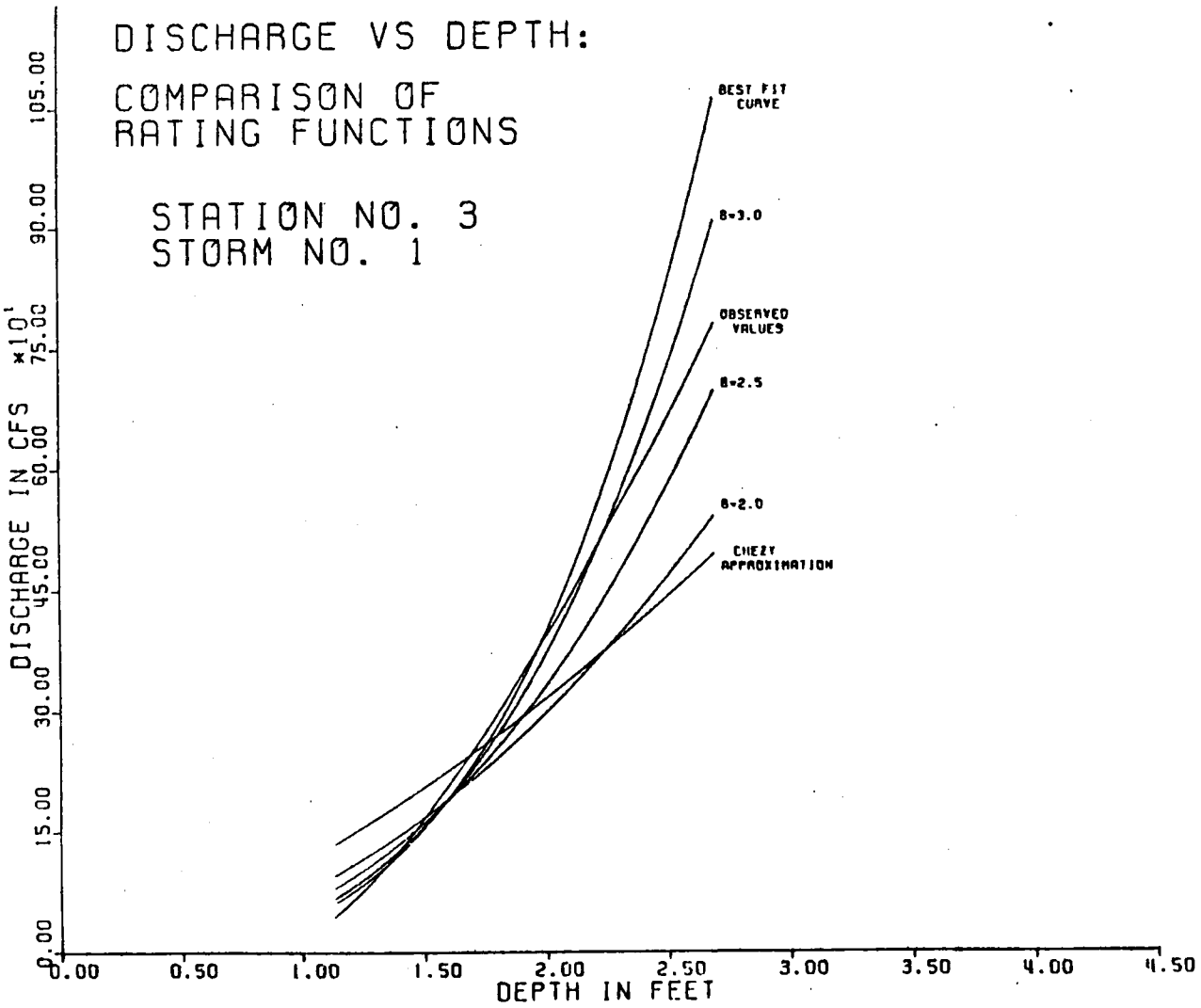


Figure 11. Comparison of Rating Functions at Station No. 3, Storm No. 1.

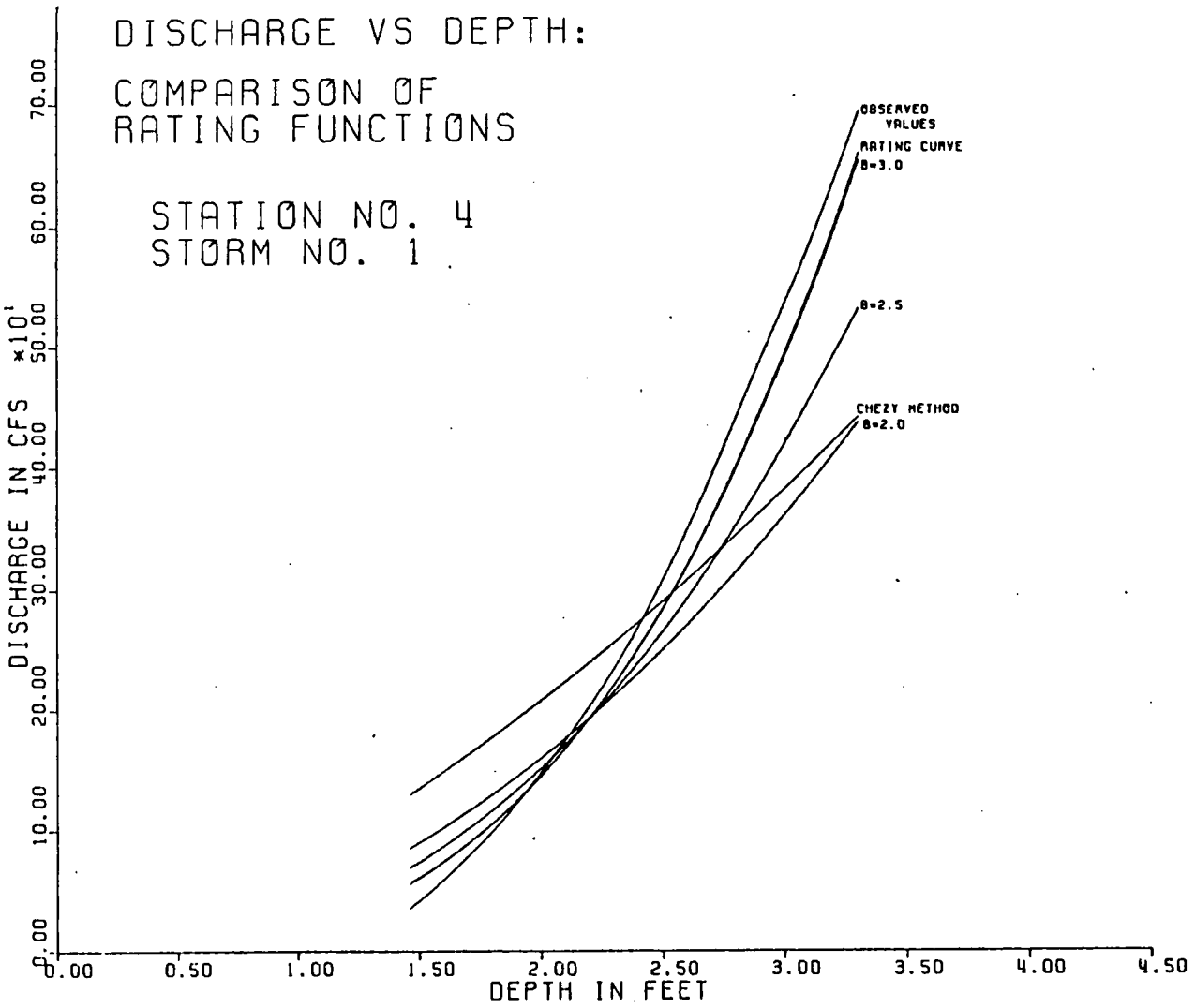


Figure 12. Comparison of Rating Functions at Station No. 4, Storm No. 1.

repeated until the downstream station was reached. Figures 13, 14, and 15 show flow profiles for all 240 2-hour time increments over the first reach during the first storm on Mahantango Creek. Each line represents one 2-hour time increment. For clarity, Figures 16 through 21 show only selected points in time for all values of b over the third reach and during both events analyzed on Mahantango Creek. It can be seen that in all cases, the downstream depth asymptotically approached the value y_n^*. This is seen to be true whether $y(0,t)$ was greater than y_n^* or less than y_n^*.

Simulation Example

In order to demonstrate the use of this model on a stream which had not been gaged as extensively as Mahantango Creek, an example simulation using the model was carried out. The West Fork Little Pigeon River at Pigeon Forge, Tennessee, was gaged continuously by the U.S. Geological Survey from 1944 to 1949. After this period, the only available data were high water marks obtained during flood events. A three mile reach of the West Fork Little Pigeon River was chosen for the simulation because of its similarity to Mahantango Creek, and because the available information for this stream is similar to that which is available for other streams.

Using the six years of data taken by the U.S.G.S., it was found that the average cross-sectional width of the stream was 70.06 feet. From a topographic map, the bed slope over the three mile reach was determined to be 0.006061 ft./ft. Bank-full depth was known to be 9.0 feet.

Based on the latest rating table (1949) from the U.S.G.S., the best fit rating curve at the downstream end of the reach is

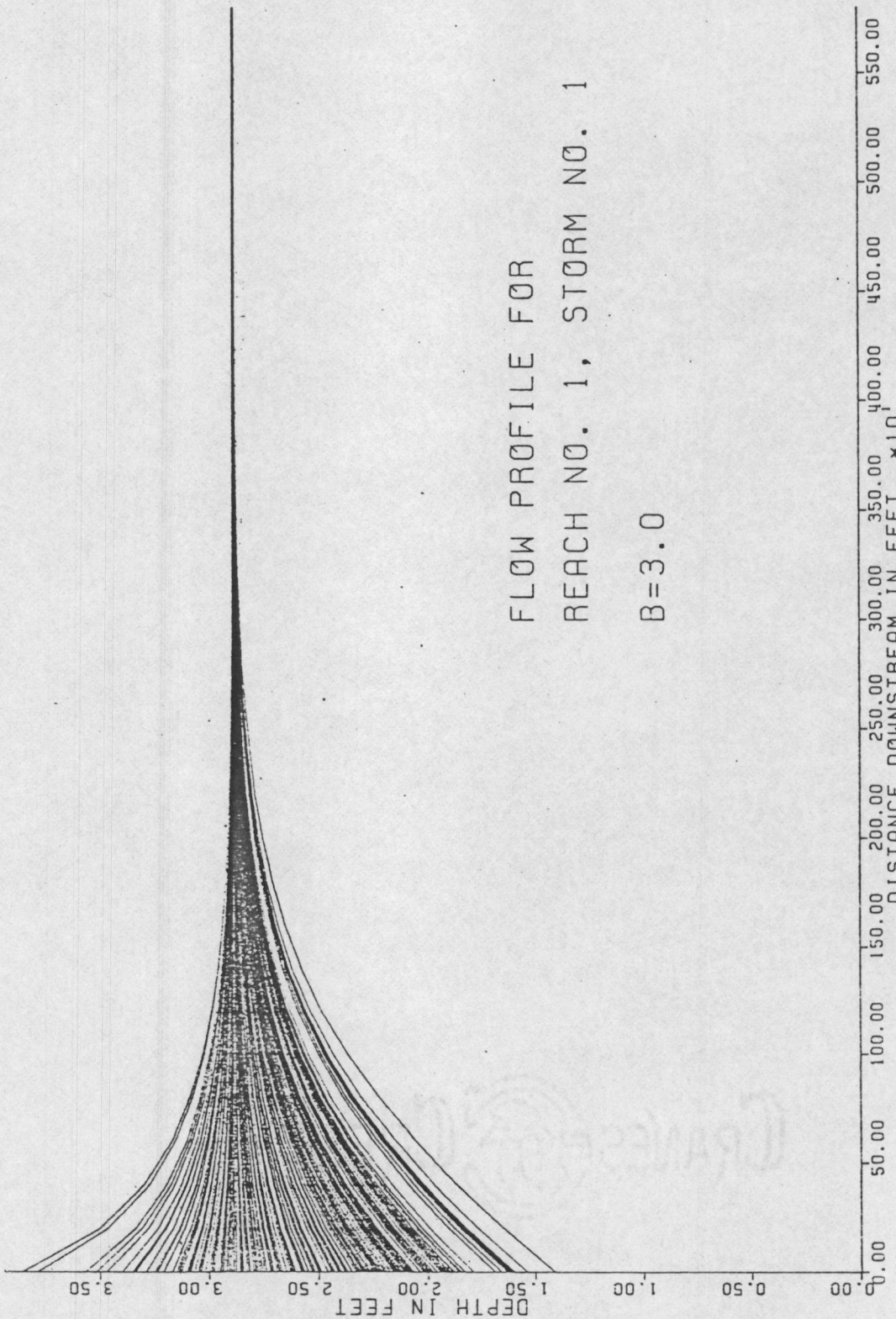


Figure 13. Complete Flow Profiles for b = 3.0; Reach No. 1, Storm No. 1.

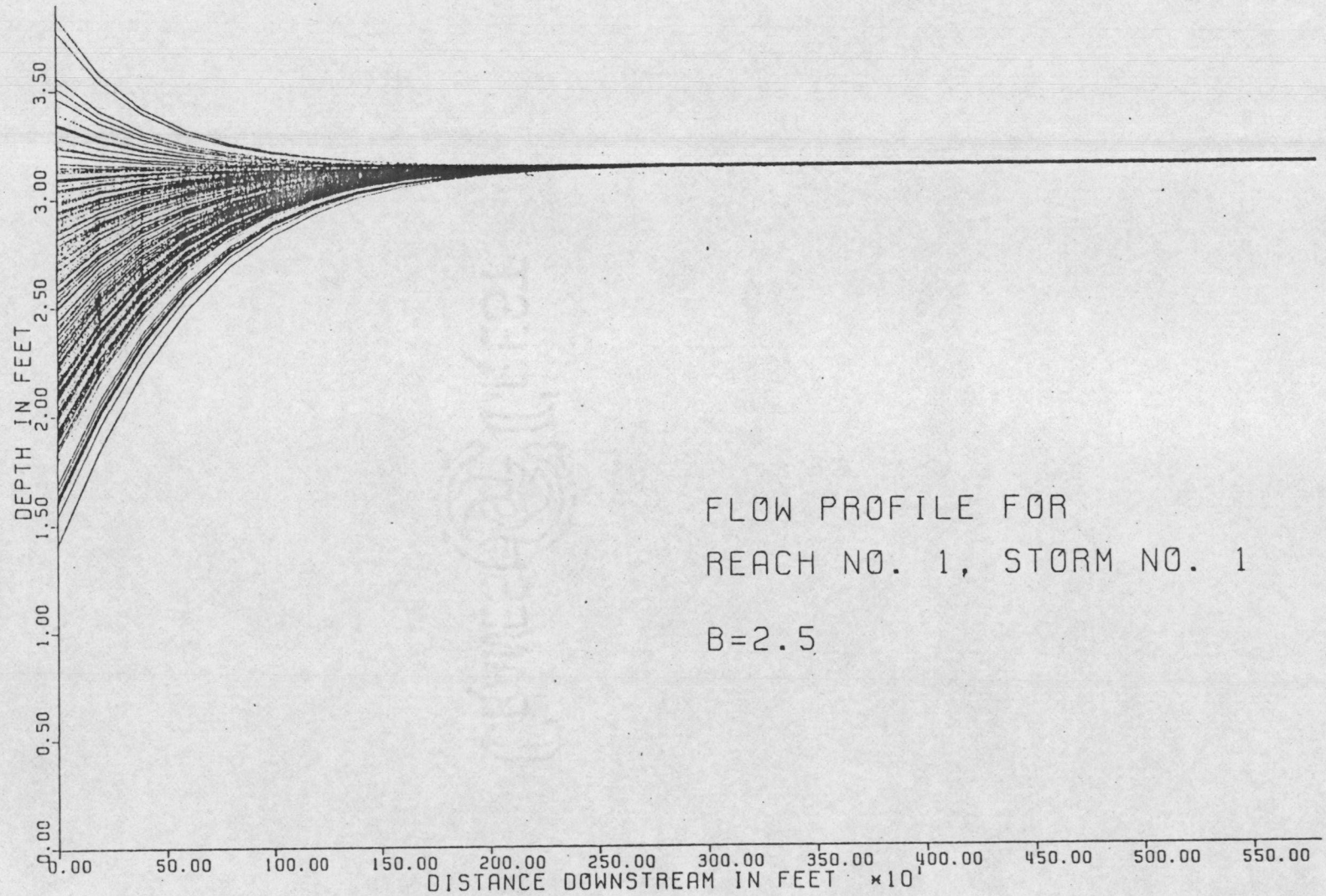


Figure 14. Complete Flow Profiles for b = 2.5; Reach No. 1, Storm No. 1.

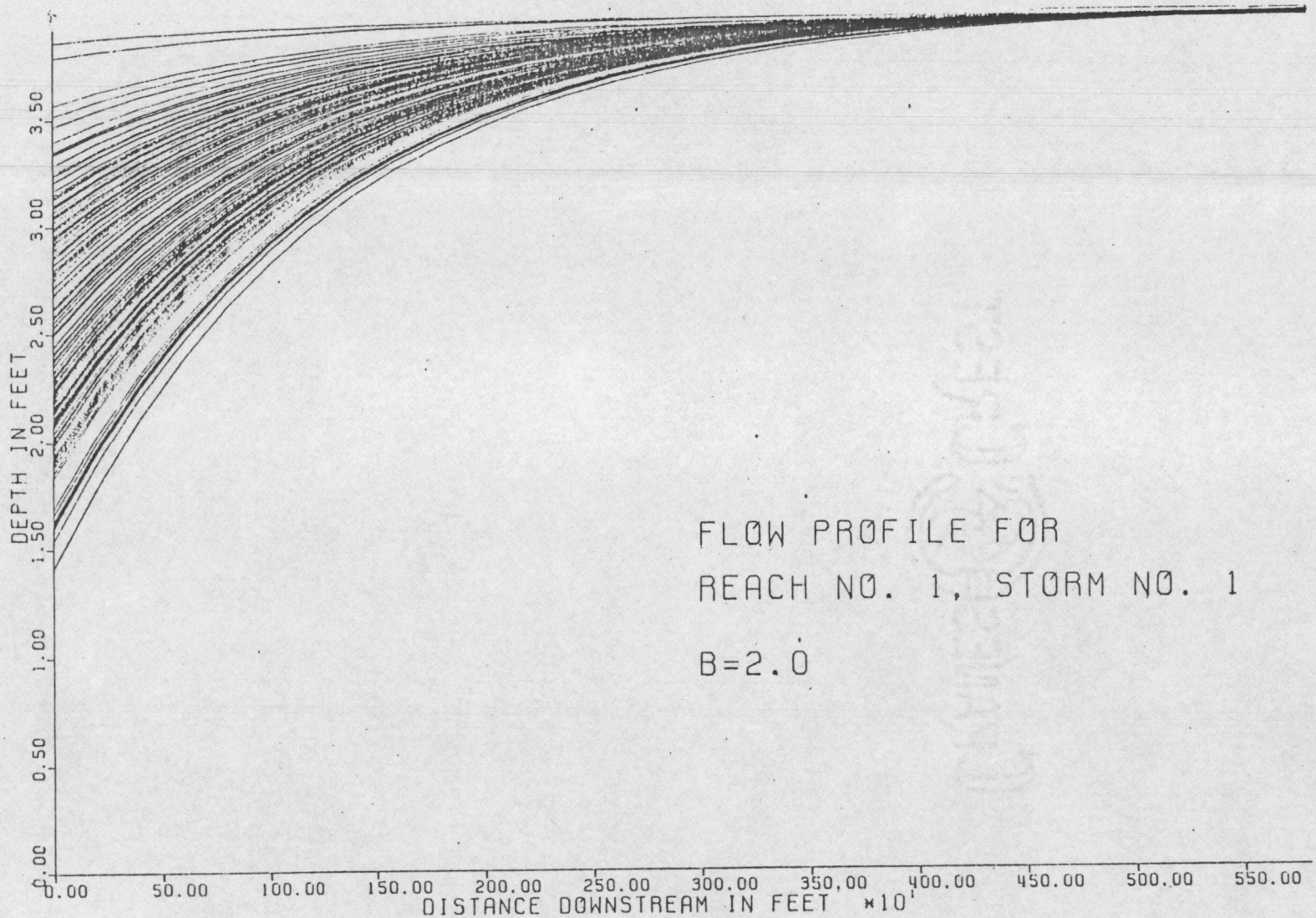


Figure 15. Complete Flow Profiles for b = 2.0; Reach No. 1, Storm No. 1.

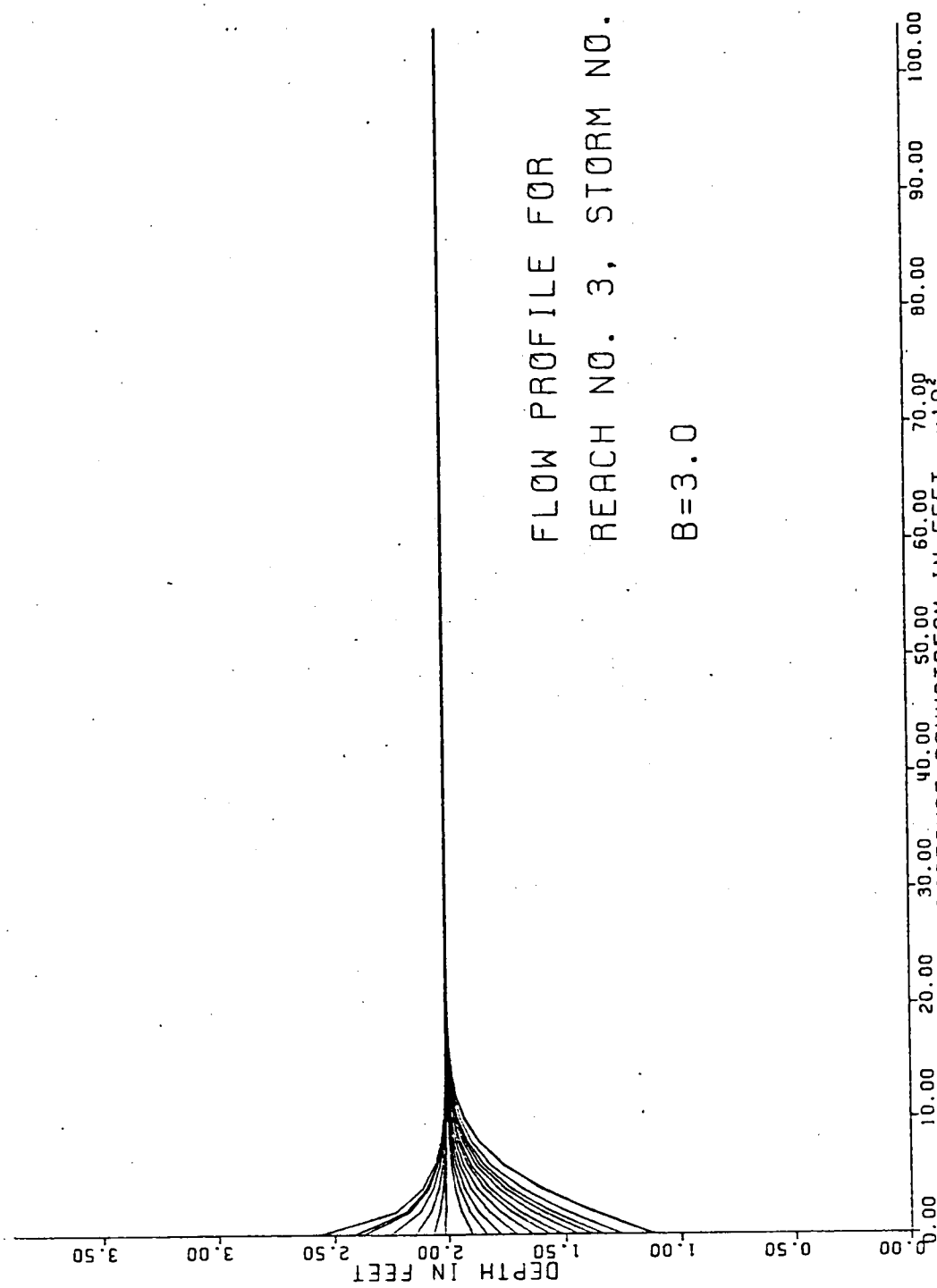


Figure 16. Partial Flow Profiles for b = 3.0; Reach No. 3, Storm No. 1.

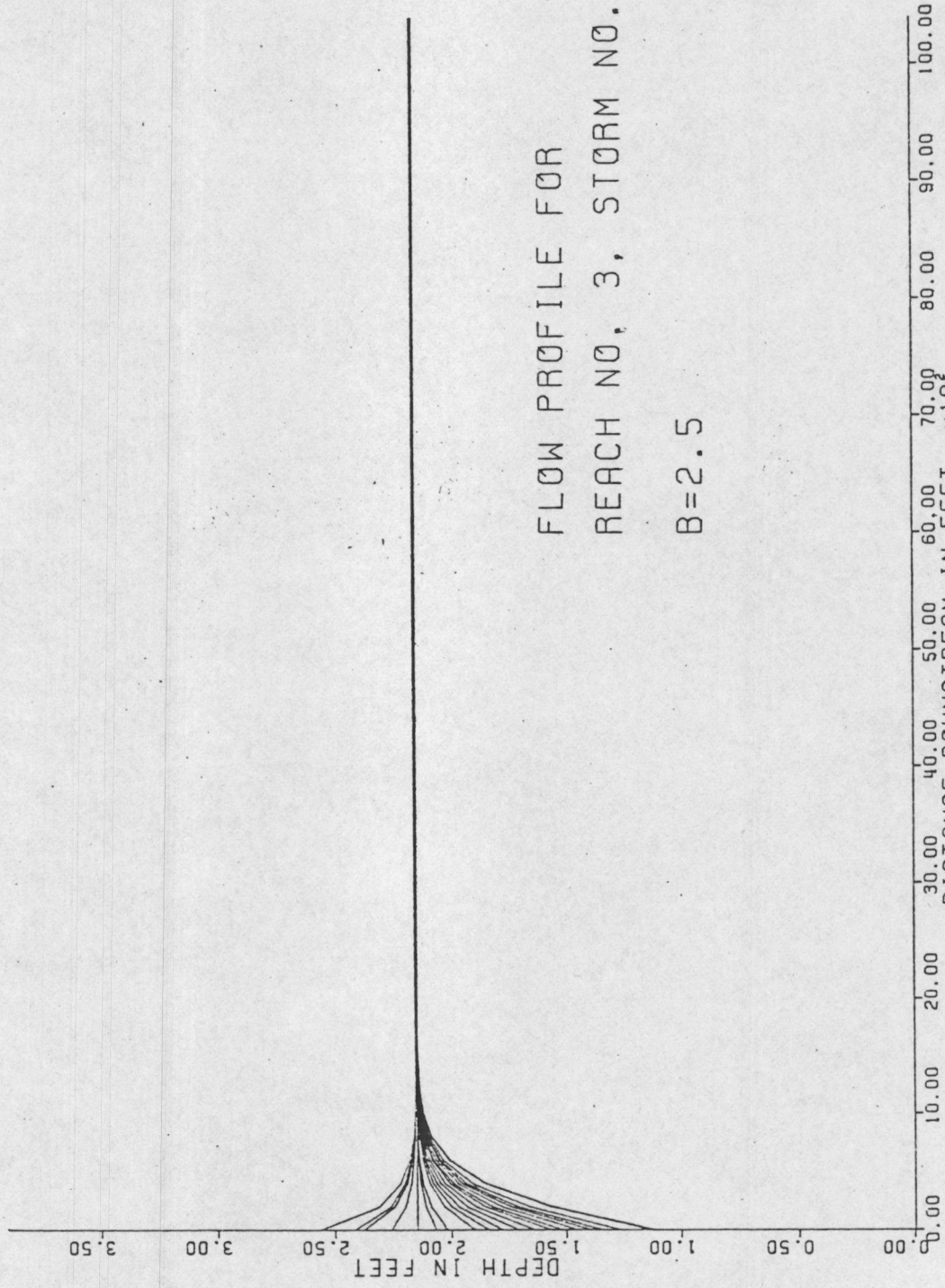


Figure 17. Partial Flow Profiles for b = 2.5; Reach No. 3, Storm No. 1.

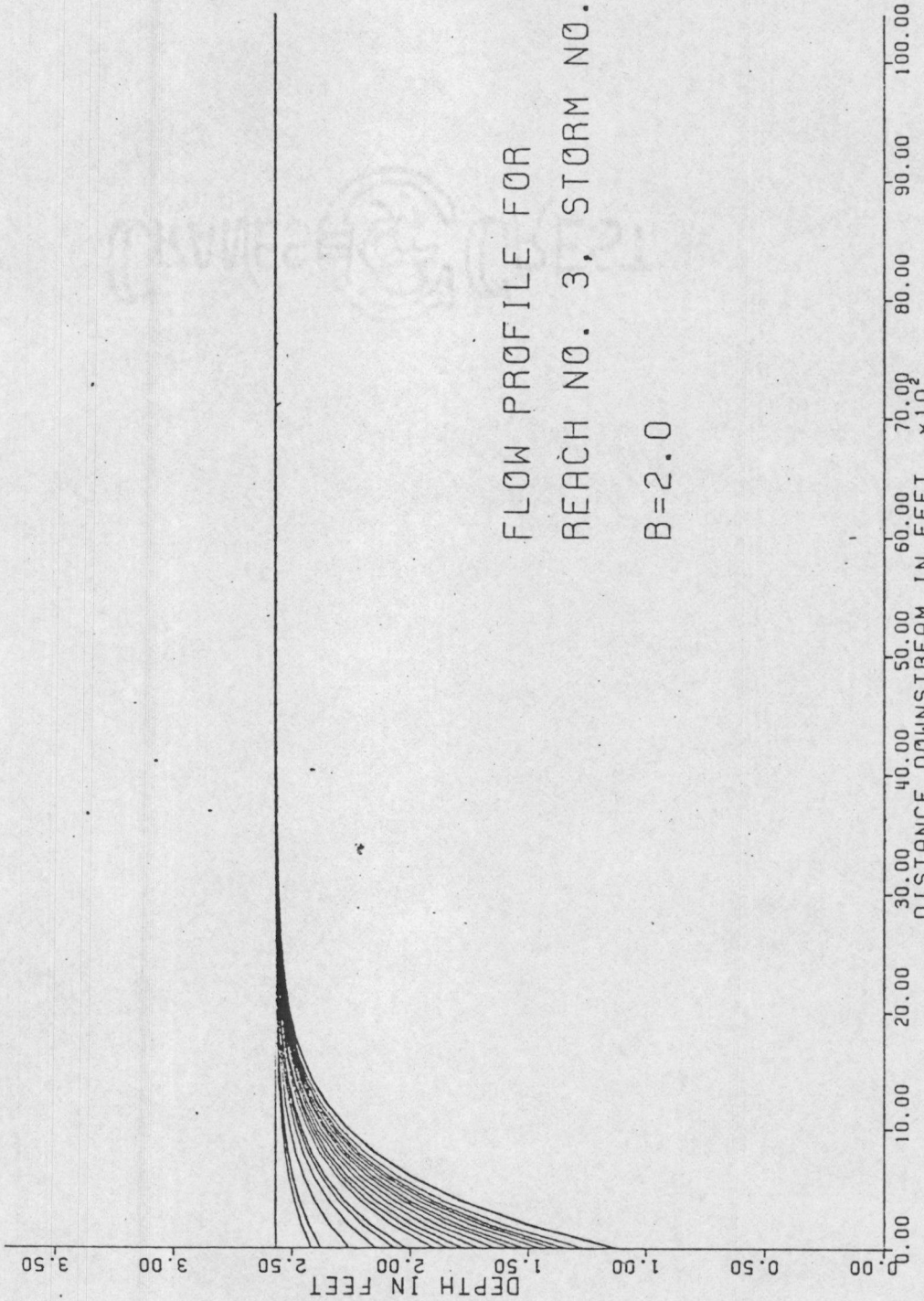


Figure 18. Partial Flow Profiles for b = 2.0; Reach No. 3, Storm No. 1.

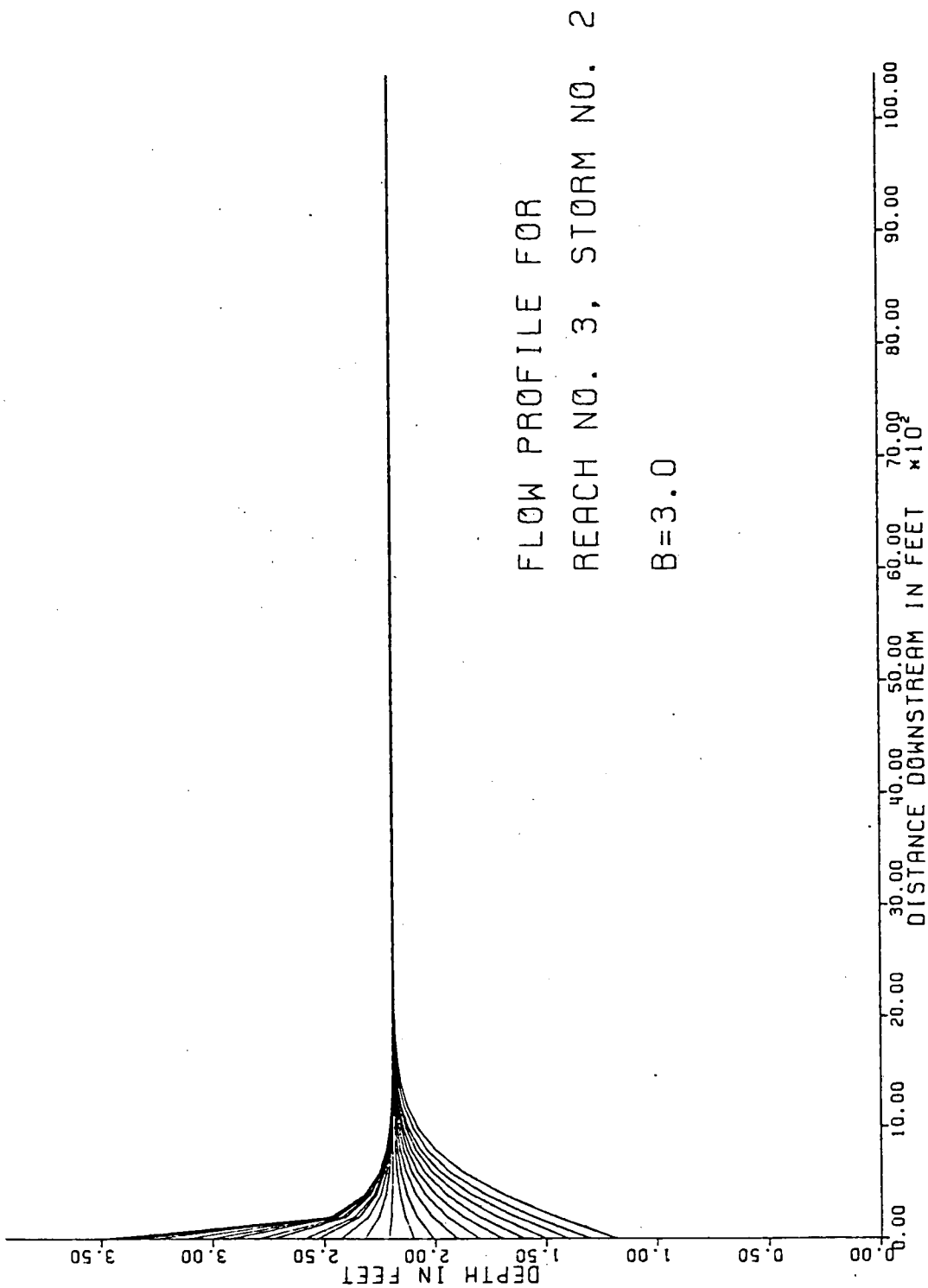


Figure 19. Partial Flow Profiles for b = 3.0; Reach No. 3, Storm No. 2.

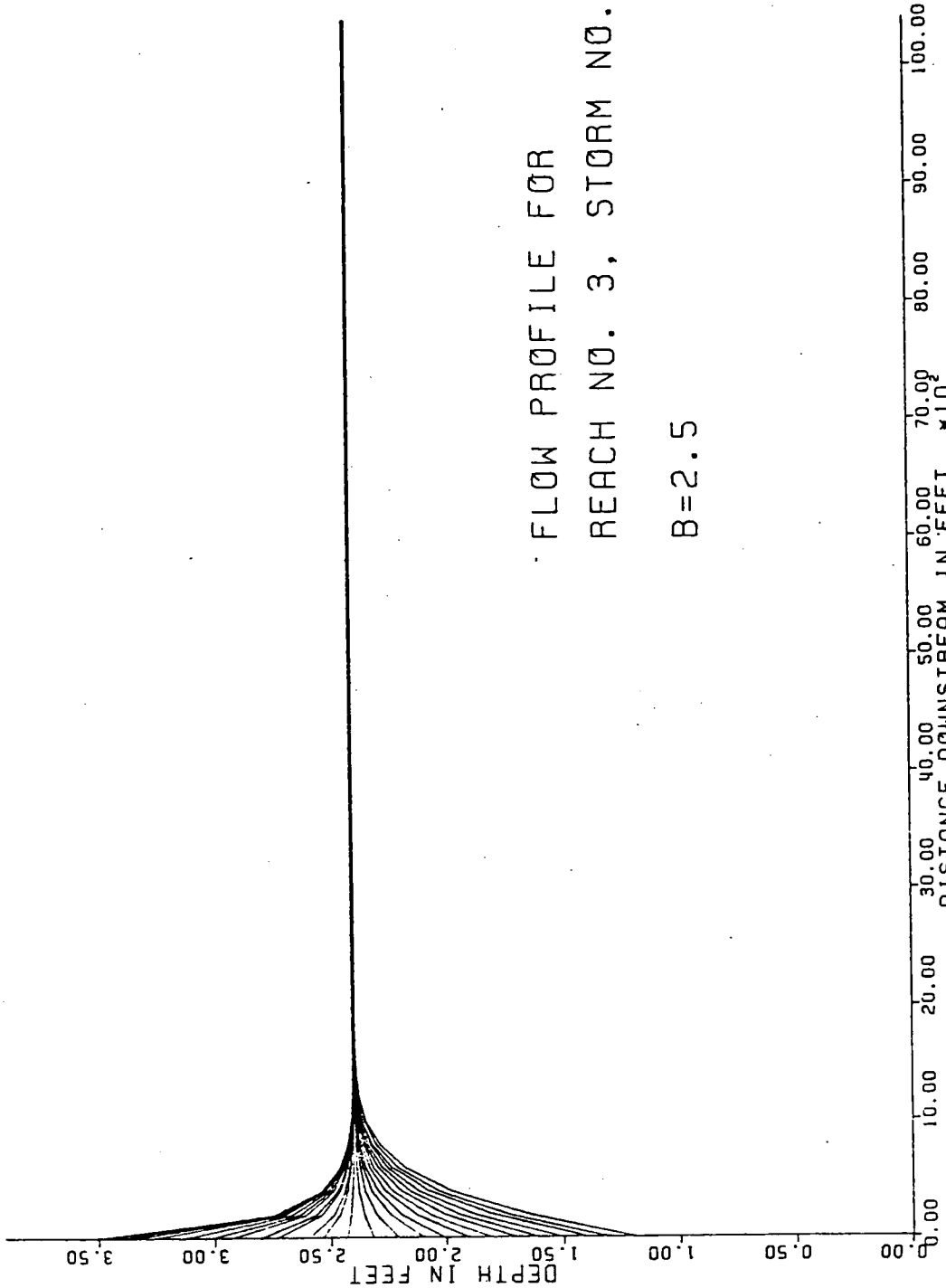


Figure 20. Partial Flow Profiles for b = 2.5; Reach No. 3, Storm No. 2.

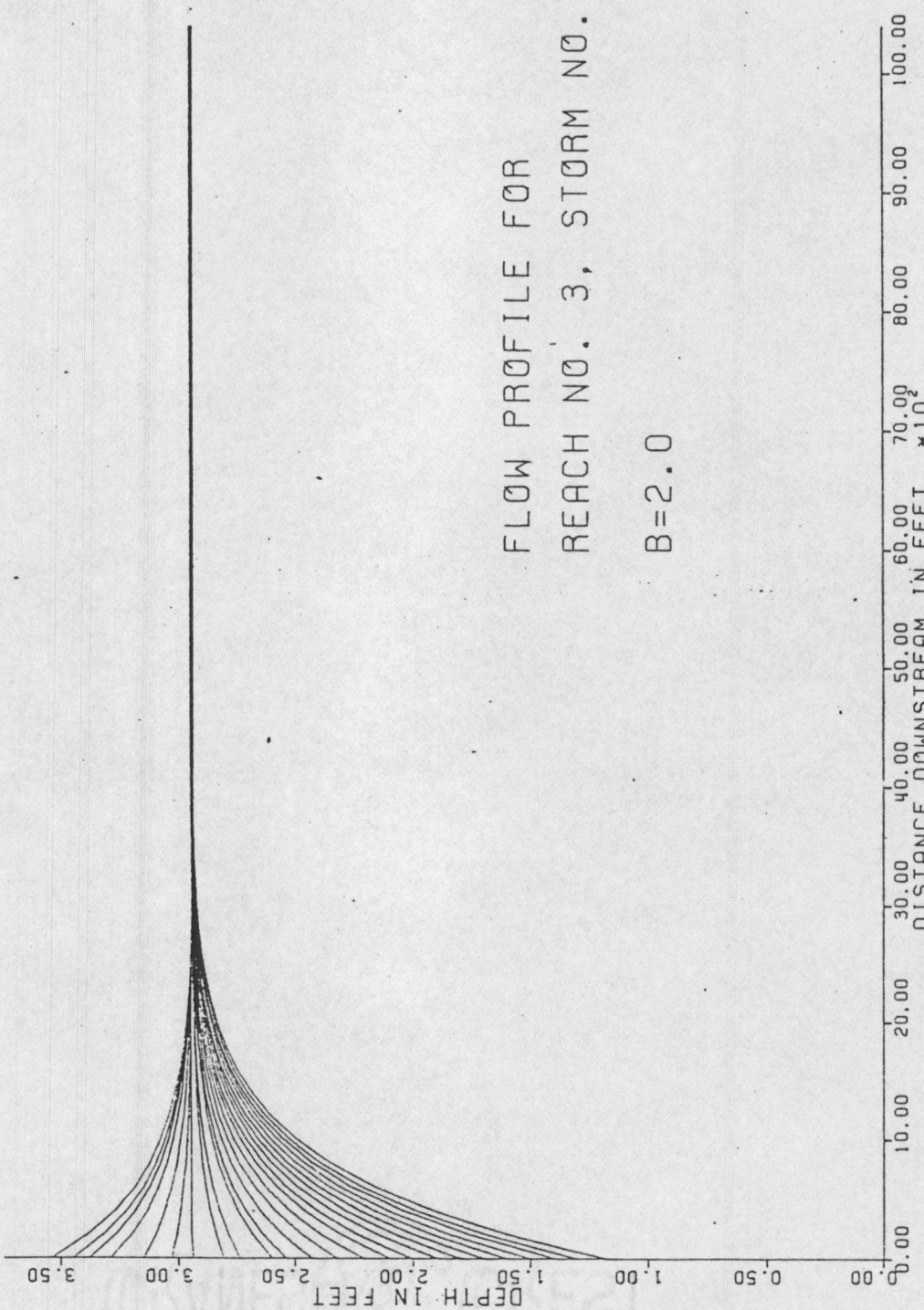


Figure 21. Partial Flow Profiles for b = 2.0; Reach No. 3, Storm No. 2.

$$Q = 19.272\ y^{2.449} \qquad (49)$$

Log stage vs. log discharge for the 1949 data is plotted in Figure 22 along with the best fit line given by Equation 49. It may be noted that the exponent on the rating curve, b, once again falls within the range of values experienced by Stall and Yang (29). From the best fit rating curve, it was determined that the kinematic streamflow solution for b = 2.5 would best simulate the actual condition of b = 2.449. Using the same procedure as was used on the Mahantango Creek data, a new A_o value was determined. The adjusted rating curve for b = 2.5 then became

$$Q = 17.873\ y^{2.5} \qquad (50)$$

The Chezy-C value was also calculated using the same method as that used in the analysis of the Mahantango Creek data. Based on the 1949 stage-discharge data, a width of 70.06 feet, a bed slope of 0.006061 ft./ft., and assuming a wide rectangular channel in which hydraulic radius may be approximated by depth, the C-value was found to be 22.19 with a coefficient of determination, r^2, equal to 0.93. Using the constant width, it also was found that the average hydraulic radius over the range of depths was 4.31 ft. while the average depth was 5.05 ft. A comparison of the rating functions used is shown in Figure 23.

The inflow hydrograph to the upstream station may be simulated using any of the available techniques, such as TENN-I (37). However in the example simulation, a simple triangular hydrograph with a peak flow equal to the bank-full condition was chosen for the routing procedure. This

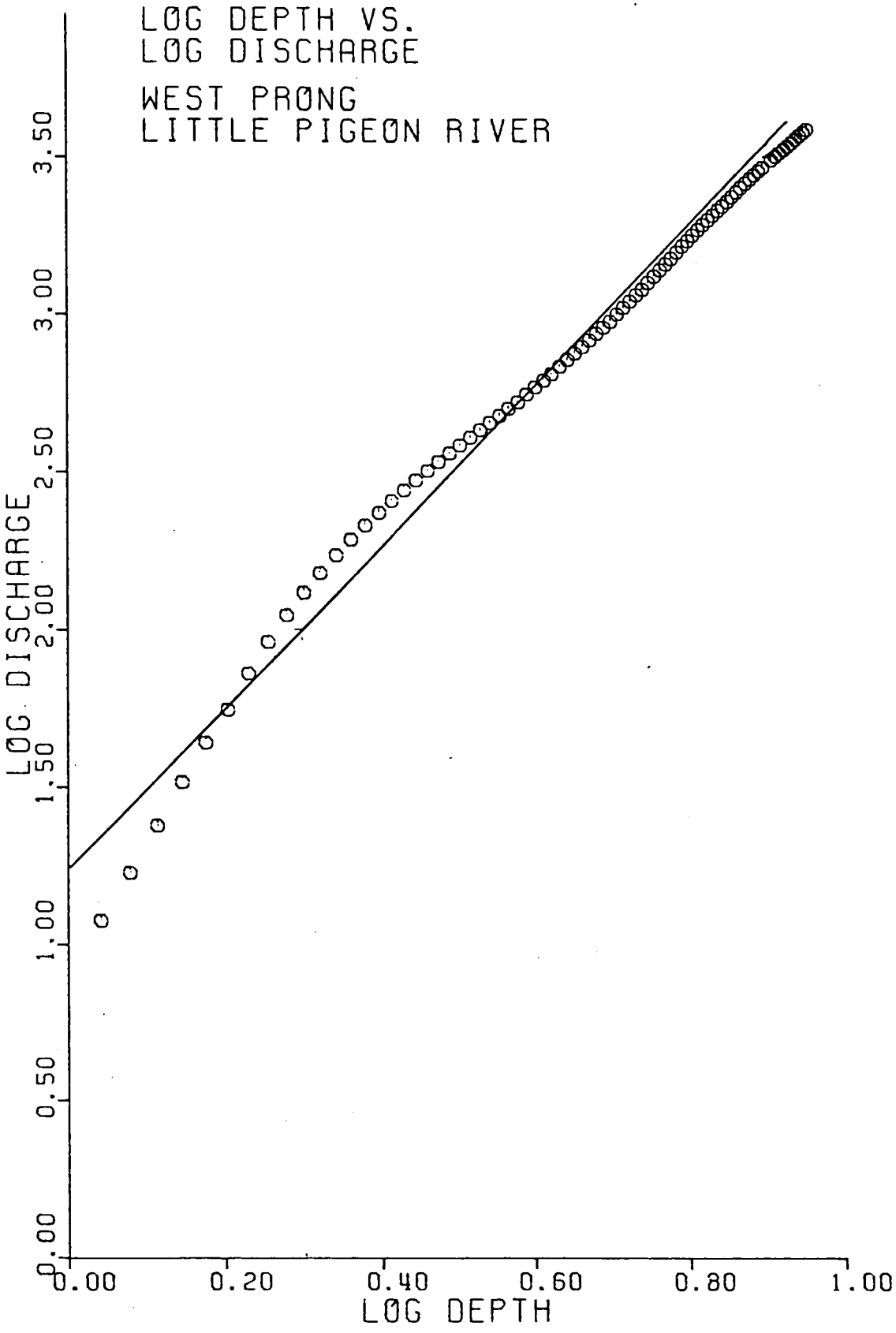


Figure 22. Log Stage vs. Log Discharge on the West Prong Little Pigeon River.

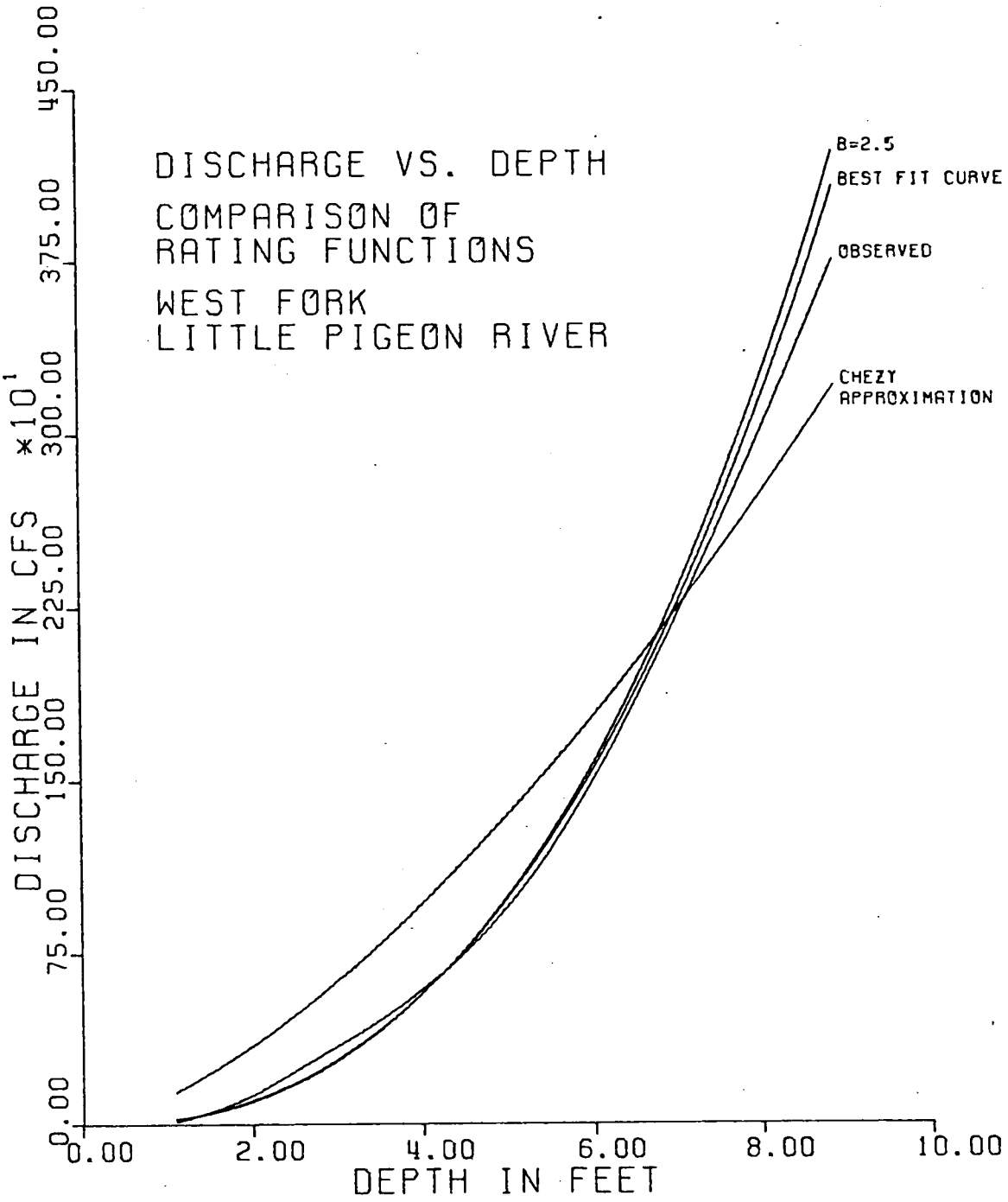


Figure 23. Comparison of Rating Functions; West Prong Little Pigeon River.

hydrograph is shown in Figure 24. Upon solving the integrated momentum equation with b = 2.5 at each time step, which was taken as 15 minutes, the resulting flow profiles were found. These profiles are shown in Figure 25.

Thus, a procedure for simulation using the three models presented may be summarized as follows.

1. From available data, determine a best fit rating function. By comparing the exponent on this rating function to 2.0, 2.5, and 3.0, determine which of the available models is appropriate for use.
2. From map data, determine the length and the bed slope of the reach through which flow is to be simulated.
3. Determine an average width of the channel cross section.
4. Using an optimization scheme such as the one used by Overton (34), determine a best fit resistance coefficient.
5. Simulate inflow to the reach by any of the accepted techniques.
6. Solve the appropriate model at preselected time and distance intervals.

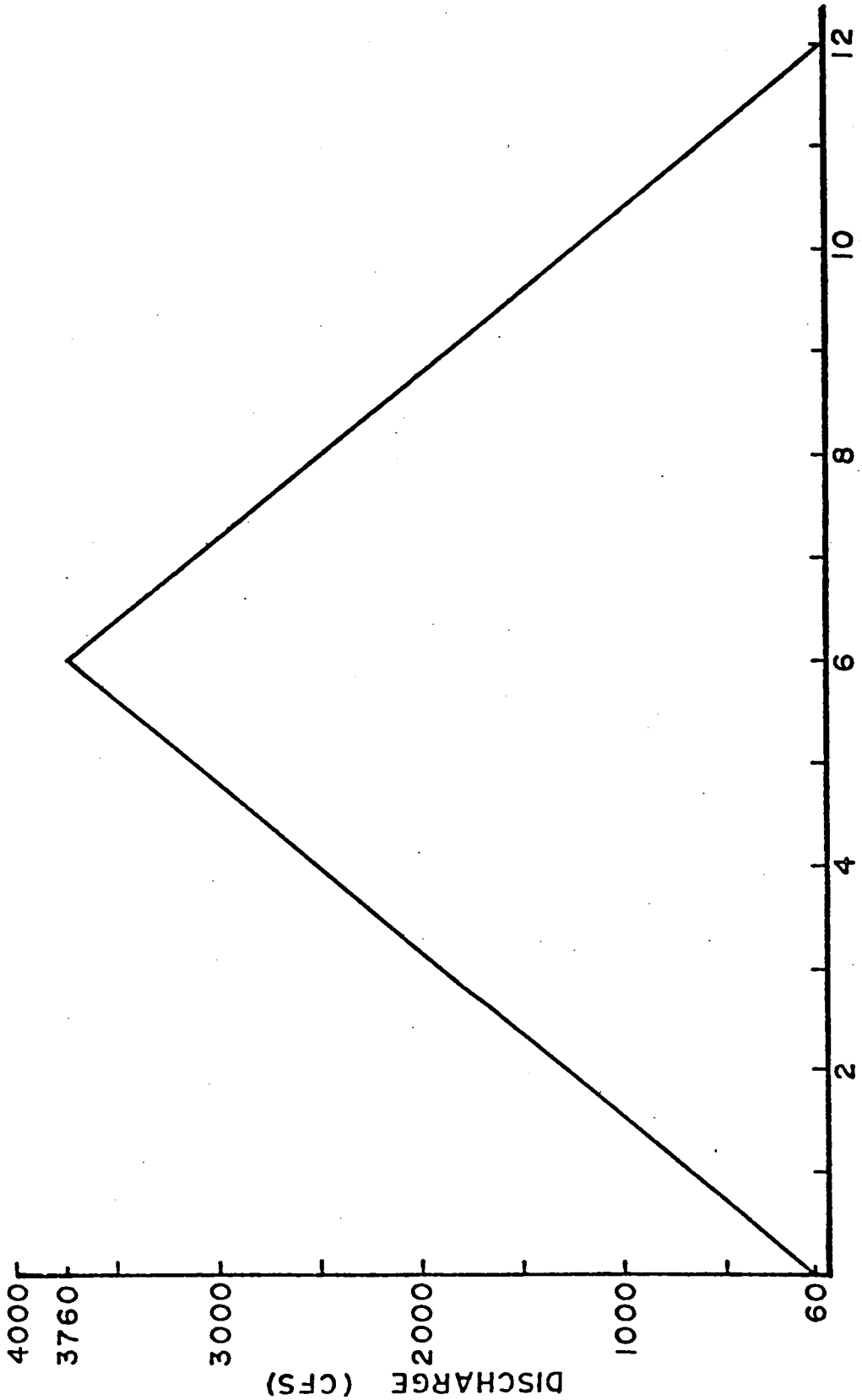


Figure 24. Hydrograph Used in Example Simulation on West Prong Little Pigeon River.

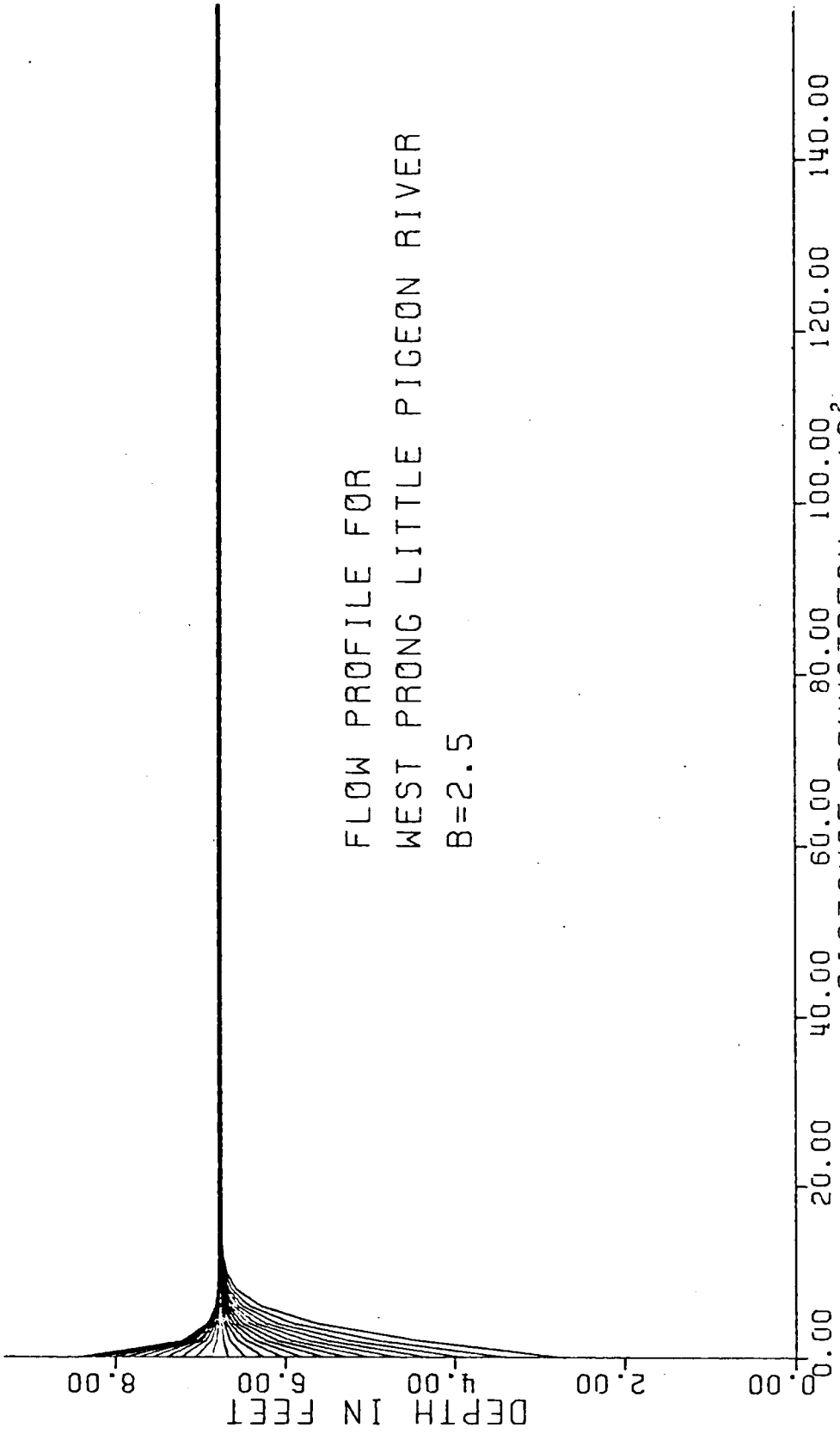


Figure 25. Flow Profiles for b = 2.5; West Prong Little Pigeon River.

CHAPTER IV

DISCUSSION OF RESULTS

Rating Curves and Resistance Coefficients

Based on the work of Stall and Yang (29) and Leopold and Maddock (25), the assumption of a b-value of either 2.0, 2.5, or 3.0 appears to be sound. Recognizing that the best fit rating curve exponents taken from Gburek and Overton's (2) study ranged from 2.74 to 3.39 (see Table 3, page 30), it would be expected that a b-value of 3.0 would best reproduce the flows which were determined by using the best fit exponents. From Table 4 (page 35), it can be seen that this is indeed true. In most cases, it can be seen that the r^2 value decreases with the b-value indicating a decrease in the ability of the adjusted rating curve (with b = 2.0, 2.5, or 3.0) to predict the actual flows. This also indicates the dependence of the models on a correctly selected b-value, i.e., one which is close in value to the best fit rating curve exponent. However, it is also evident that very little in the way of accuracy is lost by adjusting the rating curve exponents to 2.0, 2.5, or 3.0. This may be recognized by observing the comparison of the different rating functions in Figures 9 through 12 (pages 40 through 43) and noting that even the poorest fit of an adjusted rating curve to the observed values (Storm No. 2, Station Nos. 1 and 2) has a relatively good r^2 value of 0.85.

As was predicted by Leopold and Maddock, the A_o-values varied widely from station to station, but were relatively constant from storm

to storm at a given station. The variation in A_0-values is due to the change in width and depth for a given discharge between different cross sections. Thus, it can be seen that the channel cross section at each station on Mahantango Creek changed very little over the period of analysis, but there was a variation in cross sections among the 4 stations. These intimations of a variation in channel cross-section indicated by a variation in A_0 were proven by observation (2).

Thus, the requirement for a single-valued rating function with a b-value of 2.0, 2.5, or 3.0 to be used in the models has been met. The rating curves may be obtained directly by best-fitting a curve to observed values, selecting one of the 3 adjusted b-values which approximates closest the best fit b-value, and re-optimizing A_0 for the adjusted rating curve. Or, using the methods of Leopold and Maddock (25) and others, a rating curve may be simulated using the methods of hydraulic geometry.

The calculation of a resistance coefficient is a critical point in the use of these models. From the equation

$$Q = Cwy^{3/2} \sqrt{S_0} \tag{47}$$

it can be seen that C is a function of the channel width and depth of flow. Thus as the width changes, C would change; and as the depth increased, C should decrease. The assumption was made, however, that the channel width was constant over a reach, and an average width, calculated over the duration of the event at each station, was used to approximate this constant width. Obviously, any large variation from the average will result in a poor C-value. And, although C was

optimized over the range of depths encountered, no provision was made for C to vary as the depth varied.

That Equation 47, p. 37, does a poor job in predicting the observed flows can be observed in Figures 9 through 12 (pp. 40 through 43) and from the r^2 values tabulated in Table 4 (p. 35). The lack of a better fit can be attributed to the use of an average width and assuming that hydraulic radius is approximated by depth. By far, the more limiting assumption is that of a constant, average width. Yet, in spite of the poor fits, r^2 values remained above 0.83 and the C-values predicted were within the range of expected values (38).

Flow Profile Analysis

It can be recognized from Figures 16 through 21 (pp. 48 through 53) that at each time interval, the downstream depths all approach some constant value at a given station and for a given value of b. This downstream depth is seen to be y_n^*, and will hence be called the normalized kinematic depth.

From Equation 39, the normalized kinematic depth is seen to be

$$y_n^* = (CwS_o^{1/2}/A_o)^{1/(b/3/2)} \qquad (39)$$

and by definition is constant over a reach. Thus, the stipulation that C, w, S_o, and A_o be constant over a reach comes from the definition of normalized kinematic depth. However, y_n^* will be sensitive to any assumptions made in calculating C, w, A_o, and S_o. S_o may be taken accurately from either map data or actually measured, and A_o is an optimized value based on the rating curve exponent. But, the influence of the average width and average Chezy-C value is seen once again in

the term y_n^*. Since y_n^* is sensitive to C and w, and since the solutions all approach y_n^*, it is important to try to obtain the best possible width and Chezy-C values at each station to avoid the inaccuracies associated with their use.

Another possibility for inaccuracies results from the fact that the C, w, S_o, and A_o values at each station which have been averaged over times are also averaged over the length of the reach. Thus, the width for Reach No. 1, for example, is the average of the time averaged widths at Station No. 1 and Station No. 2. From Table 5 (p. 38), it can be seen that the averaging of width, Chezy-C, and bed slope between stations would result in an average value not too dissimilar from either the upstream or downstream station values. However, because of the wide range of A_o values as shown in Table 4 (p. 35), an average of the upstream and downstream values may not represent either value very well. This problem suggests that upstream and downstream stations should be chosen at points with relatively similar cross sections to avoid this possible inconsistency in the use of the models.

Table 6 shows the normalized kinematic depths for each station and each event analyzed on Mahantango Creek. It is evident from this table that the normalized kinematic depth increases as the exponent on the rating curve decreases. This value is also seen to be somewhere in the range of one half of the bank-full depth (bank-full depth for Mahantango Creek is 5 feet).

Another variation in the behavior of the flow profiles as a function of the model form can be seen in Figures 16 through 21 (pp. 48 through 53). It may be recognized that for b = 3.0 and b = 2.5, the depths

TABLE 6

NORMALIZED KINEMATIC DEPTH VALUES ON MAHANTANGO CREEK FOR EVENTS ANALYZED

Storm	b	Reach 1	Reach 2	Reach 3
1	3.0	2.88	1.99	2.01
	2.5	3.13	2.12	2.15
	2.0	3.96	2.48	2.58
2	3.0	3.14	2.14	2.18
	2.5	3.48	2.33	2.40
	2.0	4.65	2.85	3.04

of flow converge to y_n^* at around 1500 to 2000 feet downstream. For the profiles in which b = 2.0, however, it can be seen that the depths converge to y_n^* at about 3500 feet downstream.

The fact that all depths converged to the normalized kinematic depth at a short distance downstream suggests some sort of hydraulic equilibrium condition for the cases of b = 2.5 and b = 3.0. Since the physical characteristics of the channel, i.e., width, bed slope, Chezy-C, and the rating curve are all assumed to be constant along the reach; and since it was assumed that there was no lateral inflow to the reach other than the inflow hydrograph, the model seems to indicate some "normal" depth of flow. Physically, this equilibrium condition could indicate the depth of kinematic flow which is in equilibrium with the influent (or effluent) groundwater table.

In reality, this normalized kinematic depth has not been observed under storm conditions because of continuous lateral inflow and because the assumed constant physical conditions do not, of course, exist in a natural channel. Thus, the physical significance of a normalized kinematic depth of flow appears, for now at least, tenuous, at best. What is significant, however, is that these closed form analytical solutions to the kinematic streamflow equations appear to converge to some equilibrium depth value. Because the conditions under which the models were developed, i.e., the equation for the conservation of linear momentum for kinematic streamflow and the existence of a single-valued rating function, have been verified, the existence of a normalized kinematic depth should be valid under the assumptions inherent in the solution. It remains to determine the validity of the existence of a normalized kinematic depth under more reasonable assumptions.

The fact that the flow profiles do converge to a singe value at some relatively great distance downstream suggests that the models may show a greater utility on shorter reachers — reaches in length of about 500 feet. However, as the reach length on which the model may be applied decreases, any advantage which the analytical solution has over an explicit numerical solution may be lost. Thus, care should be exercised in developing more mathematically complex solution schemes which hold no advantage over less rigorously developed methods.

For conditions of no lateral inflow and constant physical characteristics it might safely be argued that the depth of flow would eventually reach some equilibrium condition. However, for the case of b = 2.0, in which lateral inflow is input at each time step, it would not be expected for all of the depths to reach some equilibrium value a short distance downstream. However, as can be seen from Figure 15, p. 47, 18, p. 50, and 21, p. 53, the model does predict that all flows will come to the normalized kinematic depth.

To investigate further the behavior of the model for b = 2.0, limiting values for x, y(0,t), and q were inserted into the model to test the behavior of the model under these conditions. Two conclusions were reached. If the term

$$1 - (2q\ A_o/w^2gS_o)$$

is less than zero, then the downstream depth, y(x,t) is predicted to increase to unreasonably large values as x increases to infinity. This would correspond to the case of very high lateral inflow. On the other hand, if the later inflow is within the normal range of values and the

$$1 - (2q\ A_o/w^2gS_o)$$

term is greater than zero, as it was in this analysis, then $y(x,t)$ always approaches y_n^*. If $y(x,t)$ is greater than y_n^*, then $y(x,t)$ remains infinitesimally greater than y_n^*. The opposite is also true.

Because the results of the model do not seem to be hydraulically or physically justifiable, it would appear that the assumptions under which the model was developed limit the model's practicality. Although mathematically correct, the physical simplifications which were made in order to obtain the closed form analytical solutions restrict the model somewhat for use as a tool to investigate the kinematic streamflow phenomenon.

Simulation Example

As expected, the model predicted flow profiles which tended toward the normalized kinematic depth for the simulation example on the West Prong Little Pigeon River. The normalized kinematic depth was found to be 6.77. Although the results from the simulation appear to have little physical significance, the simulation does show how, with a minimum amount of information, the model can be applied to a stream. As the kinematic streamflow process becomes more understood, the significance of normalized kinematic depth may be further developed. This model may then offer a method for comparison of the kinematic streamflow process among different streams.

CHAPTER V

CONCLUSIONS AND RECOMMENDATIONS

Closed form analytical solutions to the kinematic streamflow equations were shown to exist for the cases of b = 2.0, 2.5, and 3.0. These solutions have the advantage of being based on hydraulics rather than using some arbitrary method of relating inflow to outflow (39). A relatively small data requirement is also an advantage of the analytical solutions. However, severely limiting physical assumptions were made in order to obtain the solutions.

The models may be applied recursively to consecutive reaches on a stream for which there exists depth-discharge data from one gaging station per reach. In addition, a single-valued rating should exist all along the reach. The stream channel should be prismatic and approximately wide rectangular. Finally, an average bed slope, resistance coefficient, and width is required over each reach in order to apply the models.

Analysis of the results of the modeling process showed that the models predicted that flows would approach an equilibrium depth as the inflow hydrograph passed through the reach. This equilibrium depth was called the normalized kinematic depth.

From further analysis of the solutions it was concluded that it was hydraulically and physically improbable that all flows would approach this equilibrium depth, particularly when lateral inflow was a model input. Thus, it appeared that the assumptions under which the models

were derived limited the practicality of the models. It does appear, however, that the models may be applied to relatively short reaches with some degree of success. The actual distance downstream at which these models are valid should be the initial object of continued study of the kinematic streamflow phenomenon.

As the next logical step in the study of kinematic streamflow, the kinematic streamflow equations should be numerically integrated without the constraints placed on the analytical solutions. Comparison of the two forms of solution and the results of the two modeling attempts should offer further insight. However, care should be taken so that whatever utility is gained in obtaining solutions by making the simplifying assumption of the kinematic condition is not lost in the mathematical complexities required to solve the kinematic equations.

Finally, the normalized kinematic depth deserves further study. Modeling kinematic streamflow on a large number of different streams and under different flow conditions should give a basis on which to compare y_n^* values. The effect of hydraulic geometry on the normalized kinematic depth should also follow as a natural consequence of this study.

LIST OF REFERENCES

LIST OF REFERENCES

1. Lighthill, M. J., and C. B. Whitham, "On Kinematic Waves: Flood Movement in Long Rivers," Proceedings Royal Society of London, A.229, pp. 281-316.

2. Gburek. W. J., and D. E. Overton, "Subcritical Kinematic Flow in a Stable Stream," Journal of the Hydraulics Division, ASCE, Vol. 99, No. HY9, September 1973, pp. 1433-1447.

3. Overton, D. E. and M. E. Meadows, Stormwater Modeling, Academic Press, New York, N. Y., 1976.

4. Price, R. K., "Comparison of Four Numerical Methods for Flood Routing," Journal of the Hydraulics Division, ASCE, Vol. 100, No. HY7, July 1974, pp. 879-899.

5. Liggett, J. A., and D. A. Woolhiser, "Difference Solution of Shallow-Water Equations," Journal of the Engineering Mechanics Division, ASCE, Vol. 93, No. EM2, April 1967, pp. 39-71.

6. Strelkoff, Theodor, "Numerical Solution of Saint-Venant Equations," Journal of the Hydraulics Division, ASCE, Vol. 96, No. HY1, January 1970, pp. 233-252.

7. Amien, M., and C. S. Fang, "Implicit Flood Routing in Natural Channels," Journal of the Hydraulics Division, ASCE, Vol. 96, No. HY12, December 1970, pp. 2481-2500.

8. Ponce, V. M., R. M. Li, and D. B. Simmons, "Applicability of Kinematic and Diffusion Models," Journal of the Hydraulics Division, ASCE, Vol. 104, No. HY3, March 1978, pp. 353-360.

9. Hyami, S., "On the Propagation of Flood Waves," Bulletin No. 1, Disaster Prevention Research Institute, Kyoto University, Kyoto, Japan, December 1951.

10. Ponce, V. M. and D. B. Simons, "Shallow Wave Propagation in Open Channels," Journal of the Hydraulics Division, ASCE, Vol. 103, No. HY12, December 1977, pp. 1461-1476.

11. Henderson, F. M., Open Channel Flow, The Macmillan Co., New York, N. Y., 1966.

12. Quick, M. C., and A. Pipes, "Nonlinear Channel Routing by Computer," Journal of the Hydraulics Division, ASCE, Vol. 101, No. HY6, June 1975, pp. 651-664.

13. Seddon, J. A., "River Hydraulics," Transactions, ASCE, Vol. 43, Paper No. 871, June, 1900, pp. 179-229.

14. Overton, D. E., and M. E. Meadows, Streamflow Modeling, Academic Press, New York, N. Y., 1978. (in press).

15. Henderson, F. M., "Flood Waves in Prismatic Channels," Journal of the Hydraulics Division, ASCE, Vol. 89, No. HY4, July 1963, pp. 39-67.

16. Woolhiser, D. A., and J. A. Liggett, "Unsteady One-Dimensional Flow Over a Plane - The Rising Hydrograph," Water Resources Research, Vol. 3, No. 3, 1967, pp. 753-771.

17. Henderson, F. M., and R. A. Wooding, "Overland Flow and Groundwater from a Steady Rainfall of Finite Duration," Journal of Geophysical Research, Vol. 69, No. 8, April 1964, pp. 1531-1540.

18. Overton, D. E., "Kinematic Flow on Long Impermeable Planes," Water Resources Bulletin, Vol. 8, No. 6, 1972, pp. 1198-1204.

19. Schreiber, D. L., and D. L. Bender, "Obtaining Overland Flow Resistance by Optimization," Journal of the Hydraulics Division, ASCE, Vol. 98, No. HY3, March 1972, pp. 429-446.

20. Brakensiek, D. L., "Finite Differencing Methods," Water Resources Research, Vol. 3, No. 3, 1967, pp. 858-860.

21. Wooding, R. A., "A Hydraulic Model for the Catchment Stream Problem," Journal of Hydrology, (a) "Kinematic Wave Theory," Vol. 3, 1965, pp. 254-257; (b) "Numerical Solutions," Vol. 3, 1967, pp. 268-282; (c) "Comparison with Runoff Observations," Vol. 4, 1966, pp. 21-37.

22. Overton, D. E., and D. L. Brakensiek, "A Kinematic Model of Surface Runoff Response," Proc. Symp. Results of Research on Representative and Experimental Basins, Wellington, New Zealand, December 1970.

23. Woolhiser, D. A., "Overland Flow on a Converging Surface," Transactions, ASAE, Vol. 12, No. 4, 1969, pp. 460-462.

24. Kibler, D. F., and D. A. Woolhiser, "The Kinematic Cascade as a Hydrologic Model," Hydrology Papers, Colorado State University, No. 39, March 1970.

25. Leopold, L. B., and T. Maddock, Jr., "The Hydraulic Geometry of Stream Channels and Some Physiographic Implications," Professional Paper 252, Geological Survey, U. S. Department of the Interior, Washington, D. C., 1953.

26. Linsley, R. K., M. A. Kohler, and J. L. H. Paulhus, Hydrology for Engineers, McGraw-Hill, New York, N. Y., 1975.

27. Leopold, L. B., and J. P. Miller, "Ephemeral Streams--Hydraulic Factors and Their Relation to the Drainage Net," Professional Paper 282-A, Geological Survey, U. S. Department of the Interior, Washington, D. C., 1956.

28. Stall, J. B., and Y. S. Fok, "Hydraulics and Stream Geometry," Presented at the 1967 Winter Meeting of the ASAE, Detroit, Michigan, December 1967.

29. Stall, J. B., and C. T. Yang, "Hydraulic Geometry of 12 Selected Stream Systems of the United States," University of Illinois Water Resources Center, Urbana, Illinois, Research Report No. 32, July 1970.

30. Langbein, W. B., "Geometry of River Channels," Journal of the Hydraulics Division, ASCE, Vol. 90, No. HY2, March 1964, pp. 301-311.

31. Di Silvio, G., "Flood Wave Modification Along Prismatic Channels," Journal of the Hydraulics Division, ASCE, Vol. 95, No. HY3, May 1969, pp. 877-892.

33. Brakensiek, D. L., A. L. Heath, and G. H. Comer, "Numerical Techniques for Small Watershed Routing," ARS 41-113, Agricultural Research Service, U. S. Department of Agriculture, February 1966.

34. Overton, D. E., "Flow Retardance Coefficients for Selected Prismatic Channels," Transactions, American Society of Agricultural Engineers, Vol. 10, No. 3, 1967, pp. 327-329.

35. Yen, C. L., and D. E. Overton, "Shape Effects on Resistance in Flood-Plain Channels," Journal of the Hydraulics Division, ASCE, Vol. 99, No. HY1, January 1973, pp. 219-238.

36. Overton, D. E., "A Variable Response Overland Flow Model," thesis presented to the University of Maryland, at College Park, Md., in 1972, in partial fulfillment of the requirements for the degree of Doctor of Philosophy.

37. Troxler, William L., "A Stormwater Simulation Model for the Tennessee Valley," M. S. Thesis, Department of Civil Engineering, University of Tennessee, Knoxville, Tennessee, March 1978.

38. Chow, Ven Te, Open-Channel Hydraulics, McGraw-Hill, New York, N.Y., 1959.

39. Brakensiek, D. L., "Kinematic Flood Routing," Transactions, American Society of Agricultural Engineers, Vol. 10, No. 3, pp. 340-343, 1967.

APPENDIX

APPENDIX

INTEGRATION FOR b = 2.0 AND b = 2.5

Integration for b = 2.0

Beginning with Equation 35, it is seen that

$$\frac{\partial y}{\partial x} = \frac{S_o - (A_o^2 y^{2b-3}/C^2 w^2) - y^{b-2}(qbA_o/w^2 g}{1 - (b-1)^2 (A_o^2 y^{2b-3}/w^2 g)} \tag{35}$$

The substitution for b = 2 is made.

$$\frac{\partial y}{\partial x} = \frac{S_o - (A_o^2 y/C^2 w^2) - (2qA_o/w^2 g)}{1 - (A_o^2 y/w^2 g)} \tag{51}$$

Separating variables, Equation 51 becomes

$$\int \partial x = \frac{1}{(A_o/Cw)^2} \int \frac{\partial y}{\frac{S_o}{(A_o/Cw)^2} - y - \frac{2qA_o}{w^2 g}\left(\frac{Cw}{A_o}\right)^2} - \int \frac{y\partial y}{\frac{S_o}{(A_o/Cw)^2} - y - \frac{2qA_o}{w^2 g}\left(\frac{Cw}{A_o}\right)^2} \tag{52}$$

Recall from Equation 39 that y_n^* may be given by

$$y_n^* = \left[\frac{Cw}{A_o}\sqrt{S_o}\right]^{1/(b-3/2)} \tag{39}$$

Thus, for b = 2.0

$$y_n^* = (Cw/A_o)^2 S_o$$

Substituting back in Equation 52 becomes

$$\int \partial x = \frac{y_n^*}{S_o} \int \frac{\partial y}{y_n^* - y - (2qA_o/w^2 g)(y_n^*/S_o)} - \frac{C^2}{g} \int \frac{y\partial y}{y_n^* - y - (2qA_o/w^2 g)(y_n^*/S_o)} \tag{53}$$

Following the same assumptions and procedure as that shown for b = 2.5, Equation 53 becomes

$$\int \partial x = \frac{y_n^*}{S_o} \int \frac{\partial(y/y_n^*)}{1-(y/y_n^*) - (2qA_o/w^2gS_o)} - \frac{C^2y_n^*}{g} \int \frac{(y/y_n^*)\partial(y/y_n^*)}{1-(y/y_n^*)-(2qA_o/w^2gS_o)} \quad (54)$$

Assuming that $(2q\ A_o/w^2gS_o)$ is constant, and using the same assumptions and boundary conditions as for b = 2.5, the final integrated form for the case of b = 2.0 is

$$x = (C^2y_n^*/g)(U-U_o)+ [(C^2y_n^*/g)-(y_n^*/S_o) - (2qy_n^*C^2A_o/w^2g^2S_o)]^*$$

$$\log [(1-(2qA_o/w^2gS_o)-U)/(1-(2qA_o/w^2gS_o)-U_o)] \quad (55)$$

where

$$U = y(x,t)/y_n^*; \text{ and}$$

$$U_o = y(0,t)/y_n^* .$$

Integration for b = 3.0

Again beginning with Equation 35, substituting for b = 3.0, and neglecting the effects of lateral in flow, the equation becomes

$$\frac{\partial y}{\partial x} = [So-(A_o^2y^3/C^2w^2)]/[1-4(A_o^2y^3/w^2g)] \quad (56)$$

Separating variables, this becomes

$$\int \partial x = \frac{1}{(A_o/C_w)^2} \int \frac{\partial y}{\frac{S_o}{(A_o/C_w)^2} - y^3} - \frac{4C^2}{g} \int \frac{y^3\ y}{\frac{S_o}{(A_o/Cw)^2} - y^3} \quad (57)$$

From Equation 39, it can be seen that for b = 3.0, y_n^* is

$$y_n^* = (CwS_o^{1/2}/A_o)^{2/3} \tag{58}$$

Substituting this into Equation 57 and manipulating the equation as before gives

$$x = \frac{y_n^*}{S_o} \int \frac{\partial(y/y_n^*)}{1-(y^3/y_n^{*3})} - \frac{4C^2 y_n^*}{g} \int \frac{(y^3/y_n^{*3})\partial(y/y_n^*)}{1-(y^3/y_n^{*3})} \tag{59}$$

This may then be integrated to

$$x = (4C^2 y_n^*/g)(U-U_o) + [(y_n^*/S_o) - 4C^2 y_n^*/g)](\Phi-\Phi_o) \tag{60}$$

where Φ is Bresse's function and may be written as

$$\Phi = \frac{1}{6} \ln [(U^2 + U + 1)/(U - 1)^2] - (1/\sqrt{3}) \tan^{-1} [\sqrt{3}/(2U + 1)] \tag{61}$$

Φ_o is for the case of U_o and

$$U = y(x,t)/y_n^*;$$

$$U_o = y(0,t)/y_n^*.$$

VITA

Jerad D. Bales was born in Milwaukee, Wisconsin, on April 21, 1954. He graduate from Jefferson High School in 1972. In September 1972 he entered the University of Tennessee, Knoxville, and received a Bachelor of Science degree in Civil Engineering in March 1977. While at the University of Tennessee, he was employed for four quarters as an engineering co-op student with the Monsanto Chemical Company in Columbia, Tennessee. He entered the Graduate School at the University of Tennessee in April 1977, and received the Master of Science degree with a major in Environmental Engineering in August 1978.